BAŞKENT UNIVERSITY
INSTITUTE OF SCIENCE
DEPARTMENT OF MOLECULAR BIOLOGY AND GENETICS
MASTER OF SCIENCE IN
MOLECULAR BIOLOGY AND GENETICS

KNOCK OUT OF *GSH2* GENE AND PRODUCTION OF γ-GC IN *NICOTIANA BENTHAMIANA* LEAVES WITH CAS9 VECTOR/CELL PENETRATING PEPTIDE COMPLEX

BY

OĞUZHAN YAPRAK

MASTER OF SCIENCE THESIS

ANKARA – 2024

BAŞKENT UNIVERSITY
INSTITUTE OF SCIENCE
DEPARTMENT OF MOLECULAR BIOLOGY AND GENETICS
MASTER OF SCIENCE IN
MOLECULAR BIOLOGY AND GENETICS

KNOCK OUT OF *GSH2* GENE AND PRODUCTION OF γ-GC IN *NICOTIANA BENTHAMIANA* LEAVES WITH CAS9 VECTOR/CELL PENETRATING PEPTIDE COMPLEX

BY

OĞUZHAN YAPRAK

MASTER OF SCIENCE THESIS

ADVISOR

ASSOC. PROF. DR. CEYHUN KAYIHAN

ANKARA – 2024

BAŞKENT UNIVERSITY

INSTITUTE OF SCIENCE AND ENGINEERING

This study, which was prepared by Oğuzhan YAPRAK, for the program of Master of Science with Thesis (English), has been approved in partial fulfillment of the requirements for the degree of MASTER OF SCIENCE in MOLECULAR BIOLOGY AND GENETICS Department by the following committee.

Date of Thesis Defense: 19/02/2024

Thesis Title: Knock Out of *GSH2* Gene and Production of γ-GC in *Nicotiana benthamiana* Leaves with Cas9 Vector/Cell Penetrating Peptide Complex

Examining Committee Members	**Signature**
Prof. Dr. Füsun EYİDOĞAN, Başkent University	……..
Assoc. Prof. Dr. Ceyhun KAYIHAN, Başkent University	……..
Asst. Prof. Dr. Emre AKSOY, Middle East Technical University	……..

APPROVAL

Prof. Dr. Ömer Faruk ELALDI

Director, Institute of Science and Engineering

Date: … / … / ……..

BAŞKENT UNIVERSITY

INSTITUTE OF SCIENCE

YÜKSEK LİSANS TEZ ÇALIŞMASI ORİJİNALLİK RAPORU

Date: 19/02/ 2024

Öğrencinin Adı, Soyadı: Oğuzhan YAPRAK

Öğrencinin Numarası: 22110097

Anabilim Dalı: Moleküler Biyoloji ve Genetik Anabilim Dalı

Programı: Tezli İngilizce Yüksek Lisans Programı

Danışmanın Unvanı/Adı, Soyadı: Doç. Dr. Ceyhun KAYIHAN

Tez Başlığı: Knock Out Of *GSH2* Gene and Production of γ-GC in *Nicotiana Benthamiana* Leaves with Cas9 Vector/Cell Penetrating Peptide Complex

Yukarıda başlığı belirtilen Yüksek Lisans tez çalışmamın; Giriş, Ana Bölümler ve Sonuç Bölümünden oluşan, toplam 52. sayfalık kısmına ilişkin, 19/02/2024 tarihinde şahsım/tez danışmanım tarafından Turnitin adlı intihal tespit programından aşağıda belirtilen filtrelemeler uygulanarak alınmış olan orijinallik raporuna göre, tezimin benzerlik oranı %14'dur. Uygulanan filtrelemeler:

1. Kaynakça hariç
2. Alıntılar hariç
3. Beş (5) kelimeden daha az örtüşme içeren metin kısımları hariç

"Başkent Üniversitesi Enstitüleri Tez Çalışması Orijinallik Raporu Alınması ve Kullanılması Usul ve Esaslarını" inceledim ve bu uygulama esaslarında belirtilen azami benzerlik oranlarına tez çalışmamın herhangi bir intihal içermediğini; aksinin tespit edileceği muhtemel durumda doğabilecek her türlü hukuki sorumluluğu kabul ettiğimi ve yukarıda vermiş olduğum bilgilerin doğru olduğunu beyan ederim.

Öğrenci İmzası:…….

ONAY

Tarih: … / … / 20…

Assoc. Prof. Dr. Ceyhun KAYIHAN

……

ACKNOWLEDGEMENTS

I would like to express my endless thanks to my thesis advisor Assoc. Prof. Dr. Ceyhun KAYIHAN, who never withheld his support and contributions to me from my undergraduate education to my master's education, who made great efforts by following every stage of my thesis with care and meticulousness. I would like to thank my laboratory mate Halis Batuhan ÜNAL for his labor and contributions.

Finally, I would like to thank my family for always supporting me throughout my education life, for being with me in my happiness, sadness, happiness, and success

ÖZET

Oğuzhan YAPRAK

CAS9 VEKTÖRÜ/HÜCREYE NÜFUZ EDEN PEPTİT KOMPLEKSİ İLE *NİCOTİANA BENTHAMİANA* YAPRAKLARINDA *GSH2* GENİNİN KNOCK OUT EDİLMESİ VE γ-GC ÜRETİMİ

Başkent Üniversitesi Fen Bilimleri Enstitüsü

Moleküler Biyoloji ve Genetik Anabilim Dalı

2024

Gama glutamat sistein (γ-GC), terapötik ve besin takviyesi potansiyeli olan bir bileşiktir, ancak mevcut üretim yöntemleri maliyetli ve verimsizdir. Bu tez, *Nicotiana benthamiana* bitki yapraklarında gen düzenleme teknikleri ile bu bileşiği daha verimli bir şekilde üretmeyi amaçlamaktadır. Bu yenilikçi yöntemin bitki ve sağlık biyoteknolojisi alanında önemli bir parametre olacağına inanılmaktadır. *N. benthamiana* bitkilerinde γ-GC üretimini artırmak için yeni bir teknik kullanılmıştır. İlk adımda, özel olarak tasarlanmış bir CRISPR/Cas9 vektörü (pKI1.1R) ve KLA-10 hücreye nüfuz eden peptitler (CPP) kullanılmıştır. Tasarlanan gRNA, CPP-pDNA kompleksi oluşturmak için KLA-10 peptidi ile birleştirildi ve CPP-pDNA kompleksi farklı N/P oranlarında *N. benthamiana* yapraklarına infiltre edildi. Bu aşamada *Agrobacterium* tabanlı transformasyon yöntemi de kullanılmış ve seçilen yöntemin etkinliği kontrol edilmiştir. Araştırmamızda, N/P:1'in üzerindeki oranların bitki yapraklarında nekroza neden olduğu tespit edilmiştir. Hem *Agrobacterium* tabanlı bitki transformasyon yönteminde hem de geliştirilen yöntemde glutatyon sentetaz 2 (*GSH2*) geninde istenen mutasyon tespit edilmiştir. Ancak moleküler analizler tüm sonuçların karışık profilde olduğunu göstermiş ve GSH miktarında önemli bir azalma gözlenmiştir.

ANAHTAR KELİMELER: *Nicotiana benthamiana,* CRISPR-Cas9, Hücre içi giriş peptidi, Glutatyon, Gamma glutamat sistein

Başkent Üniversitesi Bilimsel Araştırma Projesi (BAP), Proje no: BAP183810

ABSTRACT

Oğuzhan YAPRAK

KNOCK OUT OF *GSH2* GENE AND PRODUCTION OF γ-GC IN *NICOTIANA BENTHAMIANA* LEAVES WITH CAS9 VECTOR/CELL PENETRATING PEPTIDE COMPLEX

Başkent University Graduate School of Natural and Applied Sciences

Department of Molecular Biology and Genetics

2024

Gamma glutamate cysteine (γ-GC) is a compound with the potential for therapeutic and nutritional supplements, but current production methods are costly and inefficient. This thesis aims to produce this compound more efficiently by gene editing techniques in *Nicotiana benthamiana* plant leaves, This innovative method is believed to be an important parameter in the field of plant and health biotechnology. A novel technique was used to increase γ-GC production on *N. benthamiana* plants. In the first step, a specially designed CRISPR/Cas9 vector (pKI1.1R) and KLA-10 cell penetrating peptides (CPP) were used. The designed gRNA was combined with KLA-10 peptide to form a CPP-pDNA complex and the CPP-pDNA complex was infiltrated into *N. benthamiana* leaves at different N/P ratios. At this stage, the *Agrobacterium*-based transformation method was also used, and the efficiency of the selected method was checked. In our research, it was found that ratios above N/P:1 caused a necrosis in plant leaves. In both the *Agrobacterium*-based plant transformation method and the method developed, the desired mutation in the glutathione synthetase 2 (*GSH2)* gene was detected. However, molecular analyses showed that all results were mixed profile and a significant decrease in GSH amount was observed.

KEY WORDS: *Nicotiana benthamiana,* CRISPR-Cas9, cell penetrating peptide, glutathione, Gamma glutamate cysteine

Başkent University Scientific Research Projects (BAP), Project no: BAP183810

CONTENTS

ÖZET iv

ABSTRACT v

LIST OF TABLES ix

LIST OF FIGURES x

LIST OF SYMBOLS AND ABBREVIATIONS xii

1. INTRODUCTION 1

2. LITERATURE 3

2.1. N. benthamiana 3

2.2. Reactive Oxygen Species (ROS) 3

2.3. ROS and Diseases 4

2.4. Glutathione 4

2.5. γ-GC 6

2.6. Genome Editing 7

2.6.1. ZFNs (Zinc Finger Nucleases) 8

2.6.2. TALENs (Transcription Activator Like Effector Nucleases) 9

2.6.3. CRSIPR/Cas9 System 11

2.6.3.1. CRISPR-Cas in bacteria and archaea 11

2.6.3.2. Parts of the CRISPR/Cas9 System 12

2.6.4. Comparison of ZFN, TALEN and CRISPR/Cas9 Systems 13

2.7. CRISPR-Cas9 System in plant biotechnology 14

2.8. Cell-penetrating peptides 15

3. MATERIALS AND METHODS 17

3.1. Bacterial strain, plasmids and Cell Penetrating Peptide 17

3.2. Bacterial culture media and culture conditions 17

3.3. Plant material and seed culture media 18

3.4. Chemicals and kits used 18

3.5. gRNA Design 18

3.6. Digestion and dephosphorylation of pKI1.1R plasmid by AarI enzyme 20

3.7. Transition of sgRNA Primers to oligoduplex structure 21

3.8. Ligation of gRNA to pKI1.1R vector 22

3.9. E. coli transformation of ligation product 22

3.10. Primer designs 22

3.11. Colony PCR 23

3.12. Agarose gel electrophoresis 23

3.13. Plasmid isolation 24

3.14. Verification of gene sequencing 24

3.15. Transformation of plasmids to Agrobacterium tumefaciens 24

3.16. Infiltration of N. benthamina leaves into the CPP-pDNA complex 24

3.17. Agrobacterium transformation to N. benthamiana plants 25

3.18. DNA extraction from N. benthamiana leaves from leaves 26

3.19. Total RNA extraction 26

3.20. Synthesis of single strand cDNA from total RNA 27

3.21. PCR after cDNA synthesis 27

3.23. Next generation sequencing of possible mutations in N. bethamiana leaves after transfection 28

3.24. Measurement of GSH amount in N. benthamiana leaves 28

4. RESULTS 29

4.1. Preparation of Plant Transformation Vector 29

4.1.1. Vector isolation 29

4.1.2. Cloning gRNA into the pKI1.1R vector 30

4.1.3. Transformation of the ligation product to E. coli 10Beta and GV3101 Agrobacterium strains …….. 31

4.1.4. Colony PCR 32

4.2. Validation of cloning by DNA sequencing 33

4.3. Mobility Shift Assay 34

4.4. Zeta Potential Measurements 35

4.5. Investigation of the prepared pDNA/CPP complex and its effects on N. benthamiana leaves after transfection 36

4.6. Comparison of N/P ratios with GFP vector 41

4.7. Investigation of the pDNA-CPP complex and the targeted GSH2 gene after Agrobacterium infiltration 45

4.8. GSH quantification 46

5. DISCUSSION 48

6. CONCLUSION 52

REFERENCES 53

LIST OF TABLES

Page

Table 2.1. Genome editing tools **……**……. 7

Table 2.2. The most widely used CPPs today and their features.....16

Table 3.1. AarI enzyme digestion and dephosphorylation protocol of pKI1.1R plasmid……..... 20

Table 3.2. Components required for Double-stranded Construction of sgRNA Primers 21

Table 3.3. Procedure for preparing annealing buffer ……..... 21

Table 3.4. Components required for ligation of the double stranded gRNA to the pKI1.1R plasmid cut with the AarI enzyme……... 22

Table 3.5. Table of primers ……..... 23

Table 3.6. Preparation table of CPP-pDNA complex in different ratios..... 25

LIST OF FIGURES

Page

Figure 2.1. Simple schematic representation of the GSH synthesis pathway in the cell ... 13

Figure 2.2. Visual schematic of the Zinc Finger Nucleases genome editing method..... 9

Figure 2.3. Visual schematic of the Transcription Activator Like Effector Nucleases genome editing method..... 10

Figure 2.4. The working principle of the CRISPR system in the bacterial system 11

Figure 3.1. Schematic image of the pKI1.1R vector ……..... 20

Figure 4.1. Growth images of *E. coli* bacteria on selective medium …….....29

Figure 4.2. Image of the isolated pKI1.1R vector in 1% agarose gel after electrophoresis 30

Figure 4.3. pKI1.1R-gRNA was transformed to 10-Beta *E. coli* strain 31

Figure 4.4. pKI1.1R-gRNA was transformed to A. *tumefaciens* strain …….....31

Figure 4.5. Post-PCR gel images of cloned but untransformed vector and transformed bacteria colonies ……..... 32

Figure 4.6. Insert specific PCR gel electrophoresis image after cloning and Transformation…….…… 33

Figure 4.7. Sequence result of the pKI1.1R vector after ligation..…… …..... 34

Figure 4.8. Gel image of mobility shift assay result ……..... 35

Figure 4.9. Zeta potential measurement of CPP-pDNA complexes prepared at different N/P ratios ……..... 36

Figure 4.10. Images of CPP-pDNA clexes prepared according to Table 3.6 on N.benthamiana leaves after 3 days post infiltration ……..... 38

Figure 4.11. Images of CPP-pDNA clexes prepared according to Table 3.6 on. N.benthamiana leaves after 6 days post infiltration …….... 39

Figure 4.12. Images of CPP-pDNA clexes prepared according to Table 3.6 on *N. benthamiana* leaves after 9 days post infiltration ……..... 40

Figure 4.13. Images of CPP-pDNA complexes prepared with *Agrobacterium* and pEAQ-GFP vector at different N/P ratios after the third day of infiltration into *N. benthamiana* leaves ……..... 42

Figure 4.14. Images of CPP-pDNA complexes prepared with *Agrobacterium* and pEAQ-GFP vector at different N/P ratios after the sixth day of infiltration into *N. Benthamiana* leaves ……..... 43

Figure 4.15. Images of CPP-pDNA complexes prepared with *Agrobacterium* and pEAQ-GFP vector at different N/P ratios after the ninth day of infiltration into *N. benthamiana* leaves ……..... 44

Figure 4.16. Images on electrophoresis gel after RNA isolation and cDNA transformation by RT-PCR using different *GSH2* gene specific primers …….....45

Figure 4.17. Gel electrophoresis images of the lower and upper bands isolated from N/P ……..... 46

Figure 4.18. Results of GSH content determination after the first, third, sixth and ninth days of CPP-pDNA complex and *Agrobacterium* infiltration prepared at different N/P concentrations …….....47

LIST OF SYMBOLS AND ABBREVIATIONS

AD	Alzheimer's disease
ATP	Adenosine triphosphate
Bp	base pair
CPPs	cell-penetrating peptides
CRISPR	regularly interspaced short palindromic repeats
DBS	double strand break
E. coli	*Escherichia coli*
GCL	glutamate cysteine ligase
GR	glutathione reductase
gRNA	guide-RNA
GS	glutathione synthase
GSH	glutathione
GSSG	glutathione disulfide
HR	homologous recombination
mM	millimolar
N. benthamiana	*Nicotiana benthamiana*
NHEJ	non-homologous end joining
PAM	protospacer adjacent motif
PCR	polymerase chain reaction
ROS	reactive oxygen species
TAE	TrisAcetate-EDTA
TALEN	transcription activator like effector nucleases
ZF	zinc finger
ZFN	zinc finger nucleases
γ-GC	γ-glutamylcysteine

1. INTRODUCTION

Disruption the balance between reactive oxygen species (ROS) generation and scavenging causes neuronal apoptosis in brain cells by promoting lipid peroxidation, protein oxidation and DNA damage. Therefore, ROS are associated with neuronal cell death in neurodegenerative diseases. Relatedly, oxidative stress due to excessive accumulation of ROS is a risk factor for the development of neurodegenerative diseases. In the brains of individuals with these diseases, assisting the antioxidant defense system is one of the therapeutic approaches. The increasing prevalence of neurodegenerative diseases and the major obstacles to the patient's quality of life make it necessary to find effective and novel therapeutic approaches, such as increasing the level of glutathione (GSH) in neurons. This is because dysregulation of GSH homeostasis and alterations in GSH-dependent enzyme activities play an important role in the induction and progression of neurodegenerative diseases such as Alzheimer's, Parkinson's, and Huntington's. Therefore, it has been proven that maintaining cellular GSH levels may help reduce the symptoms of neurodegenerative diseases.

Compared to GSH, γ-GC appears to have a higher potential for therapeutic use due to its ability to enter the cell, pass into other cells (no uptake), not be under feedback pressure and be taken orally (resistant to gastric proteases). Therefore, it has serious potential for use in chronic diseases (e.g., neurodegenerative diseases), as vitamin supplements and even as fertilizer for plants. In this context, new vitamin supplements containing γ-GC are being produced and marketed worldwide because the use of GSH in vitamin supplements is highly insufficient to increase cellular GSH. In this context, this project aims to produce γ-GC in *Nicotiana benthamiana* leaves very rapidly, in very high quantities, inexpensively, Genetically Modified Organism (GMO)-free, using current genome editing methods. Γ-GC, which will be produced locally with current biotechnological methods, has the potential to be used as a direct adjuvant drug in all diseases with increased oxidative stress levels and as a daily supplementary vitamin. Zinc-finger nucleases (ZFNs), Transcription activator-like effector nucleases (TALENs) and regularly interspaced short palindromic repeats (CRISPR) have been used to edit genomes in many species and cells, including plants, paving the way for new applications in biomedical research, medicine, and biotechnology [1,2,3]. The labor-

intensive and time-consuming protein engineering required to implement TALENs and ZFNs can be done using the CRISPR method by modifying only the RNA component (4). For the CRISPR/Cas9 system to be used in gene editing, Cas protein and guide RNA (gRNA) are needed. These components are introduced into the cell via *Agrobacterium tumefaciens* (indirect cloning method) or by transfection of plasmids encoding them. However, there are significant problems in using these two methods for plant genome editing. For example, the Cas9 nuclease gene, which is integrated into the plant genome during transformation by *Agrobacterium tumefaciens*, is very difficult to remove after the editing process in asexually reproducing plants such as bananas, grapes, and potatoes [4].

In this thesis, the CRISPR/Cas9 vector containing gRNA for the glutathione synthetase 2 (*GSH2)* gene was transfected into *N. benthamiana* leaves at different N/P ratios by CPP. Thus, the most suitable N/P ratio was determined. In addition, *Agrobacterium* transfection was performed and compared with the conventional method. It was observed that the glutathione synthetase 2 (*GSH2)* gene was mutated by editing in *N. benthamiana* leaf cells where infiltration was performed and a decrease in the amount of GSH was detected.

2. LITERATURE

2.1. *N. benthamiana*

Plants have long been recognized as a more attractive alternative to traditional expression hosts such as yeast and bacteria to produce a wide range of chemicals and biotechnological materials with medical, industrial, and research applications. This is due to its high scalability, low capital requirement for infrastructure, and the absence of pathogens and endotoxins within the scope of green biotechnology, which has recently attracted attention as a platform for protein production [5].

N. benthamiana is an Australian relative of the tobacco plant (*Nicotiana tabacum*). Its ease of manipulation through transient expression and RNA interference has made it the model plant of choice today. Its genome consists of 19 chromosomes, and it is an allotetraploid; its maternal progeny has been shown by research to be *Nicotiana sylvestris*. Although *N. benthamiana* is an endemic plant native to Australia. Thanks to the above characteristics, it is now grown in greenhouses and growth chambers of research institutions and biotechnology companies worldwide. This is due to its adoption by a much wider range of researchers, including those working on molecular plant-microbe interactions, metabolic pathways, vaccine production and synthetic biology [6].

2.2. Reactive Oxygen Species (ROS)

Our bodies' inherent metabolisms lead to minimal production of free radicals [7]. A free radical is a class of extremely reactive compounds that contains oxygen. It is defined as a set of active intermediates with a single electron that can separate electrons or atoms from other substrates and ultimately cause oxidative dissociation of the substrate. Superoxide anion (O_2•−), hydrogen peroxide (H_2O_2), and hydroxyl radical (OH•) are examples of often reactive groups. Overproduction of free radicals is thought to cause many diseases since it deactivates enzymes and activators that are engaged in biological processes [8]. Alzheimer's disease (AD) has been found to be associated with high levels of free radical production, and the degree of lipid peroxidation in AD-associated cells is utilized as a diagnostic for AD diagnosis [9].

2.3. ROS and Diseases

Pathologically, neurodegenerative illnesses are typified by apoptosis of cells and increasing dysfunction that typically impacts specific neurological systems. When morphologically analyzed, it is linked to protein misfolding, and aggregation brought on by different biological processes (gliosis). Even though brain neurons can withstand oxidative stress, certain types of neurons are more vulnerable to it; in neurodegenerative disorders, this phenomenon is known as selective neuronal sensitivity. (1) neurons need a high amount of oxygen, (2) since it is a region rich in metal ions depending on age, these metal ions play an effective catalyst role for the formation of oxidative species, (4) they are rich in polyunsaturated fatty acids that are prone to oxidation, (5) they contain low concentrations of antioxidants and related enzymes. Because of this, neurons become very vulnerable to oxidative stress. Therefore, even though it is commonly acknowledged that oxidative stress rises with age, this is a significant age-related component that increases the susceptibility of neural systems to a variety of neurodegenerative diseases, including Parkinson's and Alzheimer's diseases. Consequently, oxidative, and inflammatory damage brought on by the buildup of misfolded protein in the aged brain results in energy deficit and synaptic dysfunction. [10,11].

2.4. Glutathione

Glutathione (GSH) is a powerful antioxidant that acts as an important protector against the disruption of intracellular homeostasis as a result of redox reactions in cells. It has a wide variety of functions in cells. These are balanced functioning of the intracellular antioxidant system, maintenance of redox balance, intracellular and extracellular signaling, regulation of some enzyme activities, gene expression and cell differentiation/proliferation. GSH is the most abundant thiol-containing substance (derived from a non-protein) in any cell type and is particularly abundant in organs such as the liver and kidney. Unlike other peripheral tissues, GSH synthesis is independently regulated in the brain and is present at very low levels [12]. Conversely, brain tissue is often where oxidative stress occurs the most and yet has low levels of antioxidants or antioxidant enzymes. In addition, it is rich in unsaturated fatty acids.

The *de novo* synthesis of GSH occurs in the cytosol as a result of two consecutive ATP-dependent reactions. One is catalyzed by glutamate cysteine ligase (GCL) expressed by the *GSH1* gene to produce the GSH precursor γ-glutamylcysteine (γ-GC), and the other is catalyzed by Glutathione synthase (GS) expressed by the *GSH2* gene to combine γ-GC with glycine to produce GSH [13]. Non-allosteric feedback inhibition exerted by GSH regulates the activity of the GCL enzyme. As a result, the rate of *de novo* GSH synthesis is determined by the availability of cysteine and the activity of the rate limiting GCL enzyme [14]. During the neutralization of ROS and free radicals, GSH donates an electron; two of the resulting GSH radicals neutralize each other by forming a disulfide bond to form GSSG. Glutathione reductase (GR) then catalyzes the recycling of GSSG to GSH so that under normal physiological conditions, 98% of cellular glutathione is in the reduced form (GSH), which is not produced *de novo*. Another critical role of GSH is its function as a cysteine store. Cysteine is a precarious structure outside the cell and can be rapidly auto-oxidized to cysteine in a process that generates potentially toxic oxygen free radicals, which is highly dangerous for the cell. For this reason, the regular functioning of this pathway is essential for the cell [15].

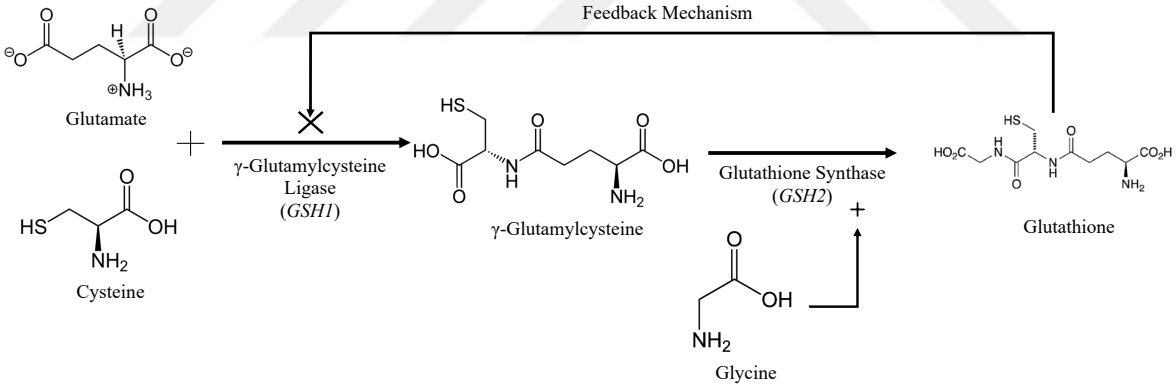

Figure 2.1. Simple schematic representation of the GSH synthesis pathway in the cell

The number of cases of age-related neurodegenerative diseases such as Alzheimer's and Parkinson's disease is high worldwide and is expected to increase exponentially in the future. Therefore, these diseases are in danger of becoming a major clinical problem. In order to cope with these neurodegenerative diseases, therapeutic agents have been developed in recent years, and studies have been carried out on their use in the treatment of these diseases. The uptake of GSH is one of these efforts, but studies have shown that the delivery of GSH

between cells is severely impaired. Passive transport of intact GSH into the cell is not thermodynamically favourable, with plasma levels between 2 and 20 μM and cellular levels between 1 and 10 mM. In addition, low cellular GSH homeostasis prevents the uptake of GSH needed to increase GSH above normal homeostatic levels directly, but studies have proposed pathways to aid active transport of GSH into the cell, specialized for several cell types, including kidney and intestinal epithelial cells [16]. In addition, studies have been conducted to modify GSH in order to facilitate its passage through the membrane. Although one of these, GSH-ethyl/ester modifications, has been shown to be much more effective than GSH in crossing the plasma membrane, the possible cellular toxicity of the metabolites formed from the de-esterification process poses a major problem [17]. As a result, glutathione generally acts as an intracellular antioxidant and redox regulator, but its intercellular delivery is not direct and free. Therefore, specialized transport systems or other mechanisms may need to be involved in situations requiring delivery between cells.

2.5. γ-GC

γ-GC is a combination of the amino acids glutamic acid and cystine and is recognized as an amino acid derivative. γ-GC is a precursor of GSH and, like GSH, actively acts as an antioxidant in cells. In addition, it acts as a rate limiter of GSH [18,19]. γ-GC has been previously reviewed as a promising therapeutic strategy to elevate GSH levels, resulting in the demonstration that the cysteine residue conserved in both γ-GC and GSH exhibits GSH-independent antioxidant properties due to the sulfhydryl group [20,21,22].

The intracellular amount of γ-GC is extremely low in the presence of GS because γ-GC is directly converted to GSH. In addition, γ-GC is a more attractive candidate for cellular uptake than GSH because it can be readily taken up into the cell either actively or passively via dipeptide transporters present in the cell membrane [23]. It can be expected that all γ-GC taken up by cells would be converted to GSH by GS, provided that glycine and ATP are not limiting. The first study on this subject was conducted by Anderson and Meister in 1983, where GSH increases were demonstrated in the kidneys of mice following intraperitoneal γ-GC administration [17]. A more recent study investigated the ability of γ-GC to modulate cellular GSH levels in primary mouse astrocyte and neuronal cell cultures, and the result of the study suggests that neurons can increase GSH production by taking up extracellular γ-GC [24].

In summary, while the age-related decrease in GSH levels has been extensively documented in the literature, the molecular processes responsible for this loss remain poorly understood. Preclinical study findings that have been published suggest that γ-GC may have a therapeutic function in the management of conditions linked to persistent oxidative stress, especially those affecting the brain. Introducing an external supply of γ-GC into the cell has the potential to elevate GSH to more optimal levels [25].

2.6. Genome Editing

Sequence-specific nucleases (ZFN, TALEN and CRISPR) are new-generation genome editing tools that have been widely used in medicine, molecular biology, and plant breeding for the last 3-4 years. Similar to DNA restriction enzymes, these nucleases cut DNA with double strands in the region of the genome where editing is desired. While these double-strand cuts are repaired through the cell's DNA repair mechanisms, HR (Homologous Recombination = Homologous Recombination) or NHEJ (Non-Homologous End Joining = Joining of Non-Homologous Ends), different modifications occur in the genome depending on which repair mechanism is used by the cell. As a result of these modifications, it causes the expression of the gene in the target region to change [26,27].

Table 2.1. Genome editing tools.

Characteristics	ZFN	TALEN	CRISPR
Study design and vector design	Difficult to design and costly	It is relatively simple but needs to be redesigned for each target.	Easy and fast to design and low cost compared to others
Target sequence length	18-24 bp	24-59 bp	20-22 bp
Target area wrong match tolerance	Mid-level	Low	High
Cutting specificity	High	High	High
Target recognition efficiency	High	High	High

A large number of genes targeting capability	None	Very low feasibility	More than one at the same time more genes can be targeted
Off-target availability	Rare off-target status	High off-target status	Mid-level off-target situation
Cutting protein	Fok I nuclease	Fok I nuclease	Cas9
Recognition site	Zinc finger motif	TALEN motif	gRNA
Repair mechanism	NHEJ and HR	NHEJ and HR	NHEJ and HR

2.6.1. ZFNs (Zinc Finger Nucleases)

ZFNs (Zinc Finger Nucleases) are the first sequence-specific nucleases designed according to the region in the genome that they want to modify. ZFNs consist of two parts, a domain and a nuclease domain, which specifically bind to DNA. The part that specifically binds to DNA consists of ZF (Zinc Finger) proteins [28]. Each unit of ZF contains 30 amino acids, which are bound to one zinc atom. Zinc finger proteins provide specific interaction of amino acids ZF proteins with DNA in various specific positions [29,30]. FokI is a cutting enzyme isolated from the bacterium *Flavobacterium okeanokoites*. This enzyme, combined with the zinc finger array, must be dimerized (just like a pair of scissors) in order to form a double-strand cut. Therefore, one monomer of the ZF protein sequence binds to the double-stranded DNA from the top, while the other monomer binds from the bottom with a 5-7 bp gap between them and forms dimers [31]. Thus, in the region between the ZF proteins bound by this upper and lower strand (which was chosen as the target site), FokI can form a double strand cut. They are repaired via NHEJ and HR as a result of the double strand cuts created by FokI in the DNA, stimulating the cell's repair pathways. While gene knock-outs are formed by repair with NHEJ, fragment integration into the genome (gene targeting) can be performed through the HR mechanism [30]. However, today, both their difficulty in design

and their toxicity due to off-target effects have made ZFNs the least preferred technique among sequence-specific nucleases [32].

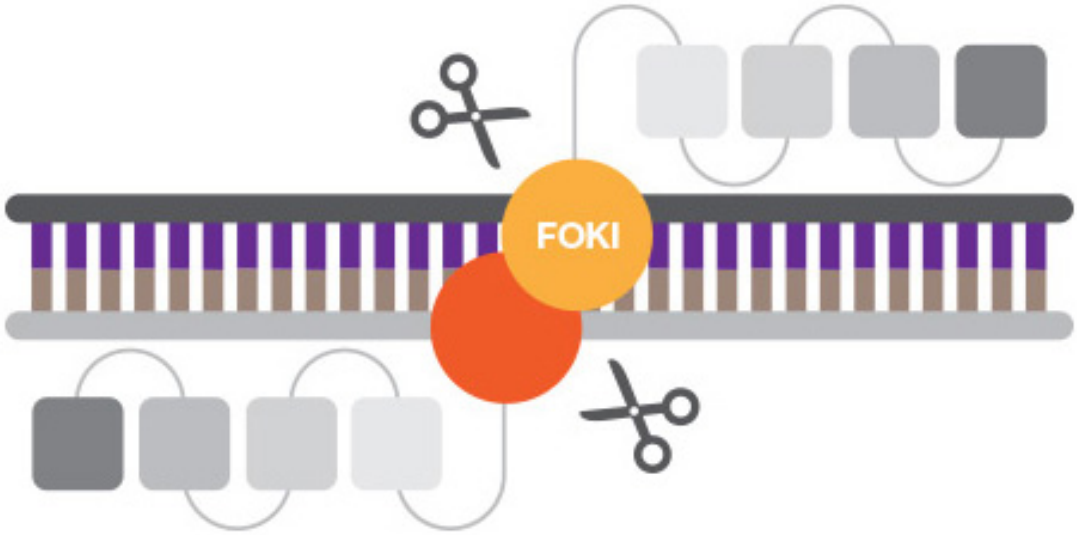

Figure 2.2. Visual schematic of the Zinc Finger Nucleases genome editing method.

2.6.2. TALENs (Transcription Activator Like Effector Nucleases)

Recently, Transcription Activator Like Effector Nucleases (TALENs) have rapidly emerged as an alternative to ZFNs for genome editing and the introduction of targeted double strand breaks (DSBs). TALENs are similar to ZFNs and contain a non-specific FokI nuclease domain fused with a customizable DNA-binding domain [29]. TAL effectors, which bind to DNA in the TALEN system, were first discovered in species of *Xanthomonas bacteria*, a plant pathogen [33,34]. During infection, bacteria belonging to the species *Xanthomonas* send transcription activator-like (Transcription Activator-Like = TAL) effectors (small molecules that selectively bind to DNA/proteins and regulate their biological activity) to the plant cells, and these effectors bind to specific plant gene promoters and activate these genes. TALENs, which are used as a genome modification tool, are created by combining the TALE protein sequence and FokI endonuclease, each of which recognizes and binds to a different nucleotide [35]. A pair of TALEN are required, which are attached to opposing DNA strands

from the lower and upper strands, which are attached to opposing DNA strands from the lower and upper strands, is required to make a cut in the desired region of the DNA. The nuclease activity of TALEN cannot occur without dimerizing (contacting each other) of TALENs that bind to the lower and upper DNA. In other words, a single TALEN does not have slaughter effectiveness on its own. There should be a 14–18 bp distance between two mutually connected TALEN structures. When this dimerized structure occurs, FokI endonucleases form double-strand cuts in the targeted DNA sequence. In addition, with the help of TALEs, it is possible to strengthen, reduce or completely stop the expression of genes. For this purpose, the segment domain is not added to the TALEN vector but is removed or inactivated. Following this, when the TALE sequence is combined with transcriptional activators or repressors and arranged in such a way that the resulting fusion protein binds to the promoter and its environment, the expression of the relevant gene can be controlled [36]. Although the specificity of the TALEN system is quite high, it has been reported that there may be off-target mutations in genome editing using TALEN [37]. TALEs without nuclease domains are used to regulate gene expression. Despite the advantages of CRISPR such as cost and easy availability, TALEN technology is due to its high specificity at the target locus [38]. Still, it is preferred by many researchers. Studies are still ongoing to develop different TALEN structures and to increase the effectiveness of TALENs by obtaining natural TALE proteins from other bacterial species [39].

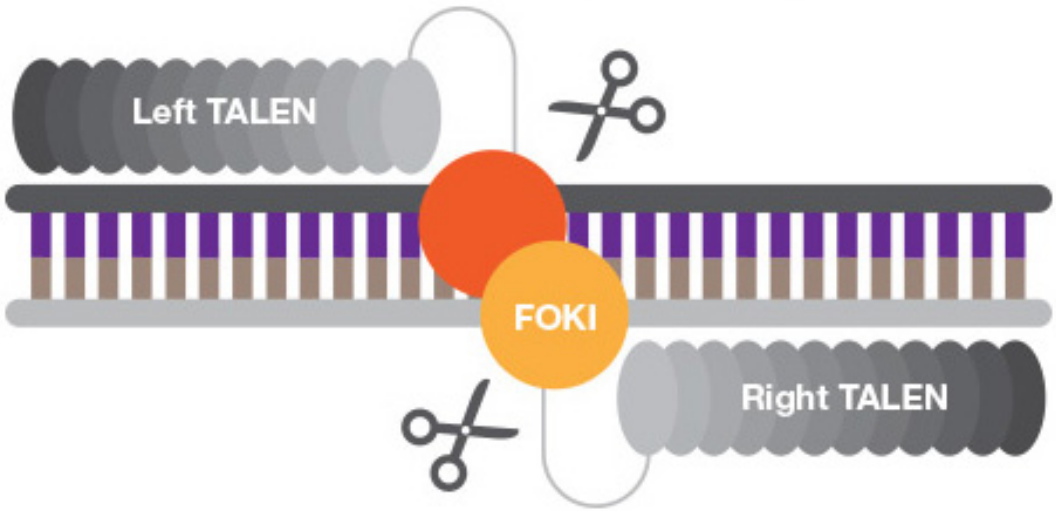

Figure 2.3. Visual schematic of the Transcription Activator Like Effector Nucleases genome editing method.

2.6.3. CRSIPR/Cas9 System

A more adaptable and effective genome editing technique has recently been designed and tested in several species, including plants, based on the bacterial clustered regularly interspaced short palindromic repeats (CRISPR)-associated protein (Cas) type II adaptive immune system. First, the CRISPR/Cas system functions as an adaptive immunity that evolved in prokaryotes over a long evolutionary history. It protects against exogenous pathogens from an invading phage or plasmid [40,41].

2.6.3.1. CRISPR-Cas in bacteria and archaea

Distant sequences of short repeats spaced by unique spacers (CRISPR loci) have long been observed in bacterial and archaeal genomes, and studies have recognized the potential of CRISPR loci and Cas proteins to provide immunity against viral and plasmid sequences. The CRISPR-Cas system is used as a gene-editing tool due to its ability to target and cleave foreign DNA [42,43,44]. 90% of archaea and 48% of bacteria have the CRISPR-Cas system [45]. While most of this system only has one copy, others may have more than one. Short sequences, or spacers, are essential parts of the CRISPR-Cas system that transduce immunity against invading pathogens and can be incorporated into CRISPR loci by the system [46]. Overall, with many forms and variants in bacteria and archaea, the CRISPR-Cas system has crucial functions as a genome editing mechanism and protection against genetic elements.

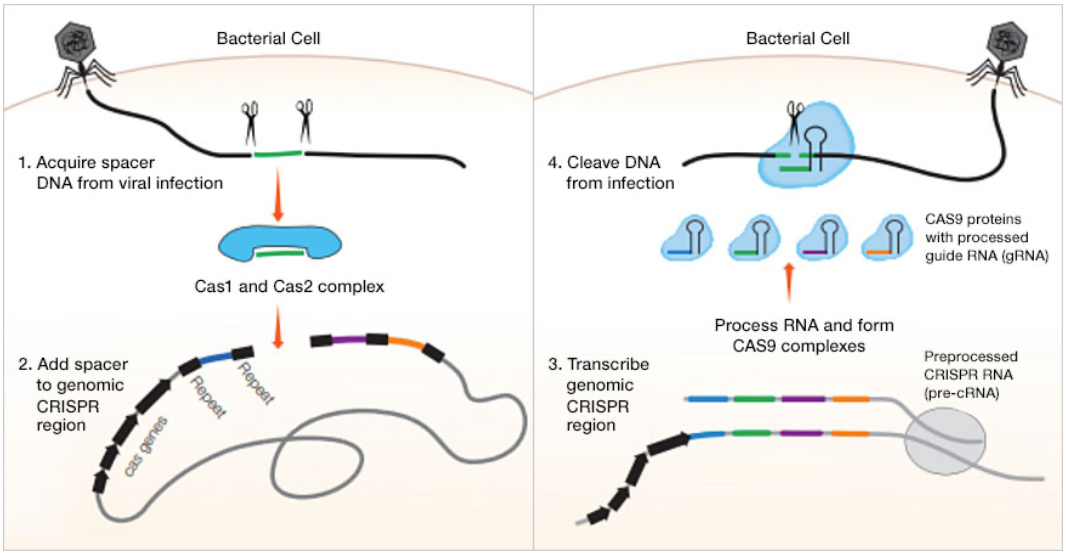

Figure 2.4. The working principle of the CRISPR system in the bacterial system.

2.6.3.2. Parts of the CRISPR/Cas9 System

The CRISPR/Cas9-mediated genome editing system requires (i) a synthetic 20 nucleotide gRNA to bind to the target site and (ii) Cas9 nuclease to cut 3 or 4 nucleotides away from the PAM sequence. Cas9 nuclease is composed of RuvC and HNH-like domains. Each of these domains binds to opposite strands to form a double strand break. There are differences between the natural and synthetic forms of the CRISPR system regarding DNA processing. For example, in the native form, gRNA and tracRNA are separate, whereas in the versions developed in the laboratory, they are combined into a single complex as sgRNA. In summary, CRISPR systems require sgRNA to bind to the target sequence, a protospace adjacent motif (PAM) at the 3' end of the target region, and Cas9 endonuclease to create breaks in the reciprocal strands.

The Cas9-sgRNA complex binds to any DNA site with a PAM sequence. If the spacer region is conjugated to the target DNA region, the Cas9 enzyme creates a double-strand break of 3 bases upstream of the PAM sequence (red arrows). If this double-strand break is error-prone, indel mutations occur at the point where the break occurs. When these mutations occur in the exon or promoter region of the gene, the gene is silenced. However, with the presence of a template during the repair of double-strand breaks, homology-directed repair (HDR) is activated, making it possible to integrate any gene into the genome [47].

The guide RNA allows Cas9 to cut a specific genomic region from among many possible loci. The binding of the Cas9 endonuclease to the target genomic locus is mediated by both the guide RNA (gRNA) containing the target sequence and a 3-base sequence known as a DNA motif (PAM) adjacent to the target sequence. For double-stranded DNA to be cut by Cas9, the 3'end of the sequence targeted by the guide RNA must contain the PAM sequence. In the absence of both the PAM sequence and the guide RNA (gRNA), Cas9 cannot bind to and cut the target sequence. Homologs of the Cas9 enzyme from different organisms or mutant Cas9s developed in various labs have different PAM sequences. Different PAM sequences allow researchers to target different genomic loci. Cas9 and its variants have 2 endonuclease domains: N-end RuvC-like nuclease domain and HNH-like nuclease domain near the protein center, the PAM interacting domain (PI). These 2 nuclease domains must be brought into the required position for Cas9 to bind to the target and cut the targeted DNA strand. Therefore, Cas9 undergoes a conformational change. While HNH cuts

the chain conjugated to sgRNA, RuvC cuts the other chain. Thus, the result of Cas9-mediated DNA damage is a double strand break approximately 3-4 bases upstream of the PAM sequence on the target DNA.

The PAM requirement limits the DNA sequences available for genome editing. Researchers are working on increasing the number of PAM sequences to make as many DNA sequences available as possible. In this sense, studies can be categorized into two categories: (1) finding new sources with different PAM requirements, this strategy is based on finding new Cas proteins, especially from different organisms, and contributes greatly to the expansion of the Cas family. (2) modifying existing PAM sequences to make them more accessible. Another part of the CRISPR system is the nuclear localization signal (NLS). The transfer of Cas proteins to the nucleus is largely dependent on this signal located at the N and/or C end of the proteins. The NLS at the 5′/3′ ends is crucial for the Cas protein to function in the nucleus in an organized manner. So far, several NLSs, such as simian vacuolating virus 40 (SV40) and nucleoplasmid, have been used in plant studies [48].

2.6.4. Comparison of ZFN, TALEN and CRISPR/Cas9 Systems

Compared to CRISPR, ZFNs and TALENs are both difficult and time-consuming to design and prepare [49]. In particular, ZFN constructs are difficult and expensive to manipulate, limiting their use in many organisms, including plants. Although TALENs are easier to construct than ZFNs, they still require experience [50,51]. The ease of preparation of CRISPR vectors and the fact that Cas9 nuclease does not need to be dimerized in order to cut are among the important advantages of this system. Based on the Watson-Crick base pairing between the target sequence and the guiding sgRNA, Cas9 identifies the target DNA. As opposed to ZFN and TALENs, this eliminates the need to prepare two distinct structures [52].

In terms of cost, the ZFN and TALEN systems are more expensive than the CRISPR system [53]. The difficulty of protein design and synthesis has prevented ZFN and TALENs from being used routinely. However, in CRISPR, modifying only 20 nucleotides of sgRNA for a different target is sufficient and does not require labor-intensive work [54]. Although TALEN is the technology with the lowest rate of off-target effects, the fact that CRISPR systems can also increase target specificity makes it a more attractive system [40].

2.7. CRISPR-Cas9 System in plant biotechnology

CRISPR/Cas 9-mediated gene editing can be used in many different fields depending on the Cas enzyme and the double chain break repair mechanism. Gene silencing is the most common application of CRISPR/Cas9 systems. This system has been successfully used to silence different groups of genes in many plant species. The most widely used CRISPR/Cas9 and other CRISPR systems cut double-stranded DNA and usually produce a double-strand break. In many cases, the double-strand break is repaired with NHEJ. When this repair system is error-prone, point mutations such as insertions or deletions occur in the gene of interest. When these mutations occur in coding regions such as exons, the gene loses its function or is silenced. Compared to T-DNA mutagenesis, CRISPR-mediated gene silencing has many advantages. The most important advantage is that gene editing is very specific. In this system, any gene can be targeted without any side effects. Therefore, the CRISPR system can quickly and accurately silence a gene in a tailored manner. This is particularly useful in studies of gene function or in eliminating the function of genes that control a negative trait.

The versatility of the CRISPR system and its superior properties compared to other methods have attracted the attention of researchers from both industry and scientific institutions, and studies on the development of products with desired properties using this system have accelerated. In a short period of time, studies were carried out on many plant species using the CRISPR system and this system was optimized for major species such as paddy, cotton, and wheat [55]. Thanks to these studies, the CRISPR system is routinely used in studies to develop plants resistant to various biotic and abiotic factors and to increase yield and quality. Stress significantly reduces the productivity of agricultural crops. Stress in plants can be divided into two categories: abiotic stress, caused by different factors such as drought, flooding, extreme temperatures, salinity, heavy metals, radiation, etc., while biotic stress includes attacks by viruses, bacteria, fungi, herbivores, and various pathogens. Mutant lines have been created in species such as paddy, tomato, cucumber, and grapefruit to provide resistance to various stress factors [56]. These lines were created using systems such as TALEN and ZFN. However, as mentioned before, these systems have significant limitations. The first studies on the use of the CRISPR system in plants were conducted in rice, wheat, tobacco, and the model plant *A. thaliana*. In wheat and paddy plants, the first

mutant plants were obtained using the CRISPR system optimized for this species, and it was understood from these studies that the CRISPR system is easy to use in plants [2]. Cas12a has several advantages over Cas9, such as requiring shorter gRNA, generating larger mutations in the target region, and assisting NHEJ-mediated DNA insertion. Again, various genetic modifications were made in plants using Cas12a and successful results were obtained [57].

Many structural and regulatory genes, including non-coding RNAs, are involved in the response of plants to different environmental stresses [58]. All these genes could be potential candidate genes for improving plant tolerance to abiotic stresses using conventional transgenic technology and currently advanced genome editing tools. However, compared to CRISPR studies for the generation of biotic stress-tolerant plants, there has been less progress in abiotic stress studies. This is mainly because there are thousands of genes that we can associate with any abiotic stress situation, and there is no single gene that plays a dominant role in this process.

Diseases and damage caused by pests and pathogens are major problems for many plant species. Biotic factors negatively affect not only plant growth and development, but also crop yield and quality, sometimes resulting in the loss of the entire crop. Plant responses to various diseases are the result of a complex mechanism. These mechanisms often require the interaction of many genes. Using transgene technology, the expression of many genes thought to be responsible for disease resistance has been increased. Nevertheless, these adjustments have been insufficient as resistance mechanisms often require the interaction of many genes. However, editing to silence genes responsible for undesirable functions often yields more effective results. Since the CRISPR system is a gene editing method, it has been effectively used to obtain mutant lines resistant to various pathogens such as viruses, fungi, and bacteria [59].

2.8. Cell-penetrating peptides

Cell-penetrating peptides (CPPs) are short peptides that penetrate the lipid layers of the cellular membrane or destabilize cellular membranes [60]. These short functional peptides can effectively transport biomolecules into animal cells and several plant cell types, including double-stranded DNA (dsDNA), double-stranded RNA (dsRNA), and large molecular weight proteins [61]. CPPs may be broadly categorized into three classes based

on their chemical structure: cationic, amphipathic, and hydrophobic. Many positively charged amino acids, including arginine (Arg) and lysine (Lys), are found in cationic CPPs. Polar and nonpolar amino acid sequences alternately make up amphipathic CPPs. Nonpolar amino acids with relatively low charges make up hydrophobic CPPs. These variations have an impact on the energy-dependent or energy-independent cellular absorption routes of CPPs. Direct translocation across the cell membrane is a component of energy-independent absorption methods, whereas endocytosis, macropinocytosis, or phagocytosis are examples of energy-dependent systems [62]. Complexes between different biomolecules and the component amino acid residues of CPPs are formed. It has been observed that the efficiency of biomolecule transport into many plant species may be increased by combining CPPs with cationic domains, such as arginine-rich, lysine-rich, and poly(lysine/histidine) domains [63].

Table 2.2. The most widely used CPPs today and their features.

Peptide no.	CPP	Amino acid sequence	Number of amino acids	Net charge at pH: 7	References
1	KLA-10	KALKKLLAKWLAAAKALL	18	5	[64]
2	BP100	KKLFKKILKYL	11	5	[65]
3	R9	rrrrrrrrr (D form)	9	9	[66]

3. MATERIALS AND METHODS

3.1. Bacterial strain, plasmids and Cell Penetrating Peptide

In this study, the plant-specific CRSPR-Cas9 vector pKI1.1R plasmid was propagated by competent cells of *Escherichia coli* strain 10-Beta (NEB). For cloning of the gRNA, the pKI1.1R plasmid was cut with the enzyme AarI at the corresponding enzyme cut site, followed by dephosphorylation (NEB) to prevent self-ligation of the sticky ends after cutting and to precisely bind the phosphorylated gRNAs specifically to that site. Ligation was performed with the T4 ligase enzyme (NEB). The pKI1.1R-gRNA plasmid was then heat shock transformed into Escherichia coli 10-Beta (NEB) competent cells. At the same time, pKI1.1R-gRNA plasmid was transferred into *A. tumefaciens* GV3101 strain by electroporation transformation method.

3.2. Bacterial culture media and culture conditions

E. coli 10-Beta cells were grown in Luria Bertani (LB) liquid medium containing selective antibiotics according to their plasmid. They were shaken at approximately 180 rpm (revolutions per minute) and incubated overnight at 37ºC in a semi-solid medium. After the plasmid was transformed into bacterial cells, competent cells were cultured in S.O.C. (Super Optimal broth with Catabolic repressor) medium. *Agrobacterium tumefaciens* GV3101 strain was grown in selective antibiotic YEB (Yeast Extract Broth) liquid medium with shaking at 180 rpm or in semi-solid YEB at 28ºC. During the preparation of semi-solid media, 1.5% (w/v) agar was added. Sterilization was performed by autoclaving at 121ºC for 15 minutes. Selective antibiotics were prepared in the required concentrations (50mg/L Spectinomycin, 50mg/L, Streptomycin, 25mg/L Rifamycin) and passed through a 0.2 μm diameter porous filter to make them sterile. Then the media were added after cooling. From colonies confirmed to carry the relevant gene, 50% glycerol stocks were prepared for long-term storage and stored in a -80ºC freezer.

3.3. Plant material and seed culture media

In the transfection studies, the model organism (*N. benthamiana*) variety was used as a bio-factory. Briefly, the seeds were placed in an Eppendorf tube containing 500 µl of 70% (v/v) EtOH, inverted for 2 minutes, and EtOH was withdrawn. 500ul of 2.5% (v/v) NaOCl was added. After 10 minutes of inversion, the NaOCl was withdrawn. Then, the seeds were washed three times for 30 seconds with 500 µl of distilled water. Micropropagation of wild-type plants to be transfected was done by culturing them in an MS (Duchefa Biochemie) medium for 3 weeks. ½ MS medium was prepared by dissolving MS and sucrose (5g for 1L) in distilled water. After the pH was adjusted to 5.7-5.8, agar (%0,07) was added, and the media were sterilized in an autoclave at 121°C for 15 minutes. All plant tissue cultures were incubated at 24±2°C, 60% humidity, and 16/8 hours (light/dark) photoperiod. At the end of 3 weeks, the plants were transferred to the medium with a mixture of potting mix (Klassman TS1) and perlite (2:1) and another 3 weeks of growth was made in the greenhouse environment and suitable growth for infiltration was reached.

3.4. Chemicals and kits used

The chemicals used in this study were provided by the Sigma-Aldrich Company (USA), Merck (Germany), Duchefa (Germany), NEB (UK) and Thermo-Scientific (Netherlands). The chemicals, enzymes, oligonucleotides and kits used in the molecular part of the experiments such as electrophoresis, polymerase chain reaction (PCR) and nucleic acid purification were mainly supplied by NEB and Thermo-Scientific. All used media and solutions were prepared with distilled water (dH_2O) or ultrapurified water.

3.5. gRNA Design

The appropriate gRNA for the *GSH2* gene of *N. benthamiana* plant was designed using CRISPRdirect tool. gRNA target sequence (yellow) and PAM sequence (red) are shown below in the coding sequence of *GSH2* gene.

>MW014352.1 *Nicotiana benthamiana* glutathione synthetase mRNA, complete cds

ATGGGCAGCGGCTATTCCTCTTCATCTTTCTCACAAAGCAGCAGCACTTTAACGCAGTG
TTGTGCTACCGTTCCTTTACAACTCCAAGAATCACACTCAAACTCTTTAAATTTCTGCT
CCGCTACTAGATTCTTGGAACCCCATCTTAATAAATCTTCCAAAATTCTAATACCCAAA
TCACCATTTTCAGCAATCTTGCCATTGAAGTGTGCTAAAAAAATGCAGACCCAAGTGG
AAGATTCTGTGAAACCCATTGTTGATCCTCATGATATTGACCCGAAATTGCTGCAGAA
ACTTTCTTATGATGCACTTGTCTTTTGCTCTCTTCGTGGTCTTGTTGTTGGTGACAGGAA
TTCAGAGAGGTCAGGAACTGTTCCTGGTGTTGGTATGGTTCATGCTCCAGTTGCTCTTT
TACCAATGTCATTCCCTGAAAGTCAATGGAGTCAAGCTTGTGAAGTTGCTCCTATTTTT
AATGAGCTCGTCGATCGTGTGAGTCAGGATGGAGAATTTTTGCAGCAATCACTCTCTA
GGACGAAAAAAGTTGATCCTTTCACCTCCAGACTACTAGAAATCCACTCCAAGATGCT
AAATATCAACAAGAAAGAGGAAATACGCTTGGGGTTGCATCGCTCAGACTATATGCTG
GATGAGCAAACTAAATTACTTCTGCAAATTGAGCTTAACACTATTTCATCATCATTTTC
GGGGCTTAGTTGTCTTGTCAGTGAGCTTCACAGGAGCTTGCTTCATCAATACAGAGAA
CGCATTGCATTAGATCCTAGCAAAATTCCCATAAACAATTCAGTAAATCAATTTGCGG
AAGCACTGGCCAAAGCTTGGAATGAATATGCTGATCCAAGGGCTGTAGTTATGTTTGT
GGTTCAAGCTGAAGAGCGCAACATGTACGATCAGCATTGGCTTTCGGCTTCACTGAGA
GAAAAACATAAAGTTATAACTACCAGAAAGACGCTAGCGGAAATTGACGCACATGGC
GAGCTTCTAGAAGATGGTACCCTCGTTGTAGATGGTGAACCAGTGGCAGTCATTTATTT
TAGAGCTGGCTATACACCAAGTGACTATCACTCGGAATCTGAGTGGAGAGCTAGGCTT
CTGATGGAGCAGTCACGTGCAGTTAAGTGCCCTTCCATTTCCTATCATTTAGCTGGGAC
CAAGAAGATTCAGCAAGAGCTTGCAAAACCCAATGTACTAGAAAGGTTTCTTGAAAA
CAAAGATGACATTGCCAAACTACGAAAATGCTTTGCAGGGTTGTGGAGTTTGGATGAG
TCCAACACAGTCAAGGATGCAATTGTGAGACCTGGCTTGTACGTAATGAAACCACAAC
GAGAAGGAGGAGGAAACAATATCTATGGGGAAGATGTGAAGGAAGCTCTTCTGAAAC
TGCAGAAGGAAGGCACTGGAAGTGATGCGTTTATACTAATGCAGAGGATTTTTCCAAC
CATTTCTCACTCGATACTAATGCGAGAAGGCATCCCTCATAAAGAACAAACCATATCA
GAACTTGGGATATATGGAACTTATTTAAGGAACGAAAAAGAAATTCTGATCAATCAAC
AGTCGGGTTACTTGATGCGGACAAAGGTCTCTTCATCAAATGAGGGTGGGGTTGCTGC
TGGTTTTGCAGCGTTGGACAGTATATACTTGGTTTGA

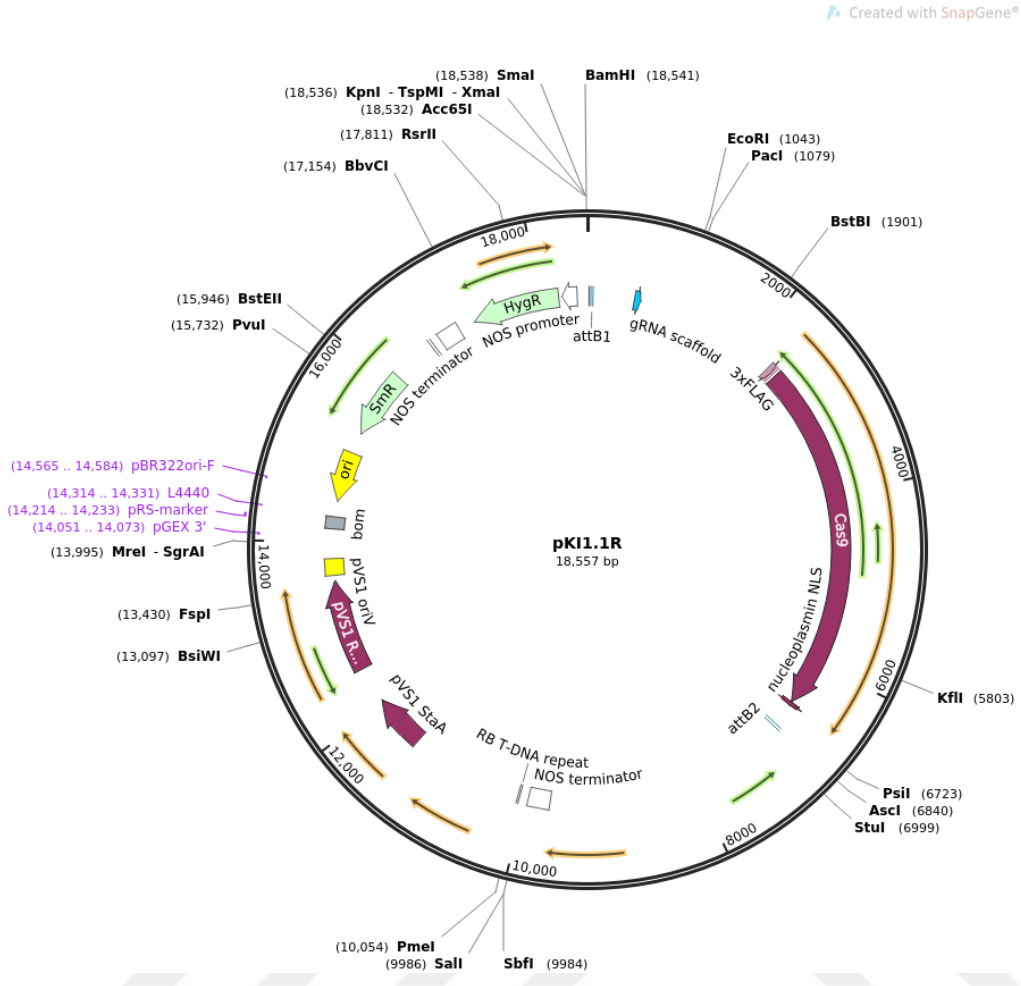

Figure 3.1. Schematic image of the pKI1.1R vector

3.6. Digestion and dephosphorylation of pKI1.1R plasmid by AarI enzyme

The pKI1.1R plasmid (Figure 3.1) was cut with AarI enzyme following the protocol below.

Table 3.1. AarI enzyme digestion and dephosphorylation protocol of pKI1.1R plasmid

Material	Volume (µL)
Nuclease-free water	2,9
10X Buffer AarI	2
DNA (vector) (0.5-1 µg/µL)	13,7
50X oligonucleotide (0.025 mM)	0,4
AarI (1U)	1
rCutSmart Buffer (10X)	2
Quick CIP	1

The mixture was incubated in a PCR for 8 h at 37°C. Immediately after the completion of the incubation, 1 µl of CutSmart Buffer (NEB) and 1 µl of Quick CIP (NEB) enzyme were added, and the PCR was set at 37°C for 30 minutes, 80 minutes at 80 °C for 2 minutes at 4°C and the cutting products were dephosphorylated.

3.7. Transition of sgRNA Primers to oligoduplex structure

Designed to complement the targeted gene region, gRNAs are synthesized as a single-stranded primer. These primers must be oligoduplexed to be cloned into a double-stranded plasmid. For this, the following protocol was followed.

Table 3.2. Components required for double-stranded construction of sgRNA primers.

Material	**Volume (µL)**
10 pmol oligo 1 (from 10 µM gRNAR)	1
10 pmol oligo 2 (from 10 µM gRNAF)	1
10X Annealing buffer	5
dH2O	43

Table 3.3. Procedure for preparing annealing buffer.

Annealing buffer: 10 mM Tris pH 8.0, 50 mM NaCl, 1mM EDTA
10X (1ml):
100ul 1MTris pH 8.0
100ul 5MNacl
20ul 500 mM EDTA
780ul ddH_2O

The prepared tubes were kept at 95 °C for 5 minutes using a PCR device and then adjusted to decrease by 1°C every minute until they reached 25 °C.

3.8. Ligation of gRNA to pKI1.1R vector

The following protocol was used to ligate of double-stranded gRNAs to pKI1.1R plasmid cut with AarI enzyme.

Table 3.4. Components required for ligation of the double stranded gRNA to the pKI1.1R plasmid cut with the AarI enzyme.

Material	Volume (µL)
T4 DNA Ligase Buffer (10X)	2
Vector DNA (18kb)	5,2
Insert DNA (24 bp) (from 20 fmol)	3
Nuclease-free water	8.8
T4 DNA Ligase	1

The reaction was gently mixed by pipetting up and down and microfuged briefly. It was then kept overnight at 16°C. It was then kept at 65°C for 10 minutes for enzyme inactivation.

3.9. *E. coli* transformation of ligation product

After mixing the 10-beta *E. coli* (NEB) cells without damaging the cells thawed on ice until the last ice crystals disappeared, 50 µl of cells were taken on ice to an Eppendorf tube. 5µl of pKI1.1R plasmid concentration of 1 pg was added to the cell mixture. The mixture was left on ice for 30 minutes. Then, to apply a heat shock, it was kept at 42°C for 30 seconds and immediately left on ice for 5 minutes. The mixture was taken to an S.O.C growth medium and incubated at 37°C at 200 rpm for 3 hours. It was then spread on the prepared selection plate (50 mg/L Spectinomycin) and incubated overnight at 37°C.

3.10. Primer designs

Primers were designed using the NCBI primer design tool and were produced by the Oligomer Biotechnology company through service procurement.

Table 3.5. Primers used in this project.

Primer names	Primer sequences (5'- 3')
GSH2 gene specific primer F	CACTTTAACGCAGTGTTGTGCTA
GSH2 gene specific primer R	TGTTTTTCTCTCAGTGAAGCCGA
Hygromycin F	CGAAAAGTTCGACAGCGTC
Hygromycin R	GGTGTCGTCCATCACAGTTTG
Cas9 F	AGACCGTGAAGGTTGTGGAC
Cas9 R	TAGTGATCTGCCGTGTCTCG
gRNA-F	**ATTG**GTCGATCGTGTGAGTCAGGA
gRNA-R	**AAAC**TCCTGACTCACACGATCGAC

3.11. Colony PCR

Colony PCR was performed to screen the bacterial cells to which the ligation product was transferred. Colonies growing on a selective antibiotic medium were taken with a sterile pipette tip, dissolved in 50 µl sterile distilled water and used as molds in the PCR reaction. The chemicals used in PCR and their concentrations are shown in table 3.5.

3.12. Agarose gel electrophoresis

Electrophoresis was used to separate PCR amplicons and DNA or RNA isolates or nucleic acid fragments. The agarose gel was prepared at a rate of 1-2% (w/v) depending on the fragment length to be imaged and using 0.5X Tris Acetate-EDTA (TAE). Ethidium bromide, added after boiling and cooling in the microwave and allowed the fragments to be seen under UV, was added to the gel solution with a final concentration of 0.4 µg/ml. For the samples to be loaded into the gel to be visible during electrophoresis, 6X loading dye (NEB) was mixed with the samples and the mixture was loaded into the wells after the gel solidified. The samples were carried out under an electric current of about 100 V for about half an hour. Gels were displayed on the imaging device.

3.13. Plasmid isolation

Plasmid isolation from *E. coli* cells was performed according to the recommended procedures using the Monorch® Miniprep Kit (NEB catalog no: T1010S). At the end of the process, plasmid DNA attached to the spin column was collected by dissolving it in 30-50 µl elution buffer (EB).

3.14. Verification of gene sequencing

The sequence of the gRNA gene found in the pKI1.1R plasmid isolated from colonies with plasmids confirmed by colony PCR was confirmed by sequence analysis before infiltration into plant leaves. Sequence analysis was performed by Intergen Genetics (Turkey).

3.15. Transformation of plasmids to *Agrobacterium tumefaciens*

A. tumefaciens GV3101 cells were transformed using the Gene Pulser® II Electroporation System (Bio-Rad). To do this, GV3101 cells were first immersed in ice, and the pKI1R-gRNA plasmid content dissolved in 1 µg (4-8 µl) of water was added to the bacterial suspension. After gentle stirring, the mixture was incubated in ice for 5 min and placed in pre-cooled 0.1 cm electroporation cuvettes (Bio-Rad). The conditions of the electroporation are as follows: 1200 Volt, 200 resistance, 25 capacitance. After applying during electroporation, 1 ml of liquid YEB medium was added to the cuvettes and the mixture was transferred to the 2 ml tube immediately afterwards. The cells were incubated at 28°C and 180 rpm for 4 hours, then precipitated by centrifugation at 3000 *g* for 10 min and redissolved in 100 µl medium. Bacteria were spread to the YEB semi-solid medium where selective antibiotics were present and incubated at 28°C for 3 days. The colony was selected by PCR using the primers listed in Table 3.5. Glycerol stocks were prepared from colonies with the relevant plasmid, including gRNA, and stored at -80°C for transformation.

3.16. Infiltration of *N. benthamina* leaves into the CPP-pDNA complex

The cloned pKI1.1R-gRNA was amplified in *E. coli* and then purified using GenElute HP Plasmid Maxiprep Kit (Sigma, Germany).To prepare peptide-pDNA complexes, 0.5 g/L

peptide was mixed with pDNA solution (approximately 1.0 mg/mL) at 25°C in various N/P ratios (0.5, 1, 2, 5 and 10). This ratio is the ratio of the number of phosphate groups (P) in the DNA molecule to the number of positively charged groups (N) in the amine group. Here N/P ratio means the number of amine groups from the peptide/number of phosphate groups from the pDNA. The final pDNA concentration was 25 µg/ml. The final concentrations of KLA-10 are summarized in Table 3.6. The prepared CPP-pDNA complexes were measured with a zeta potential meter (Zetasizer Nano- ZS; Malvern Instruments, Ltd., Worcestershire, UK).

Table 3.6. Preparation table of CPP-pDNA complex in different ratios.

For 100 µl Solution			
N/P ratio	**Stock Vector pDNA Solution (25µg/ml) (µl)**	**Final Cons. KLA-10 (µl) ****	**dH_2O (µl)**
0	25	0	75
0,1	25	0,27	74,73
0,5	25	1,35	73,65
1	25	2,7	72,3
2	25	5,4	69,6
5	25	13,5	61,5
10	25	27	48
	*** From 100µg/ml**	**** From 1mg/ml**	

Approximately 100 µl of CPP-pDNA complex solutions prepared at different N/P ratios were infiltrated directly through the lower epidermis of young *N. benthamiana* leaves of the same surface area size at approximately 1 month of growth, not yet flowering, using a needleless syringe.

3.17. *Agrobacterium* transformation to *N. benthamiana* plants

The *Agrobacterium* GV3101 strain carrying the plasmid with the relevant gRNA was grown overnight in a YEB liquid medium by shaking at 180 rpm. When the OD600 value of the culture reached 0.6, the bacteria were precipitated at 3000 g at room temperature for 10 min, their supernatants were discarded, and the remaining bacterial pellet was dissolved with 25 ml of infiltration medium. Then, using a needle-free syringe, infiltration was performed from the lower region of the *N. benthamiana* leaves from the region away from the veins.

3.18. DNA extraction from *N. benthamiana* leaves from leaves

DNA isolation from candidate plant leaves after 3-6 and 9 days of transgenic infiltration was performed using cetyltrimethylammonium bromide (CTAB). The leaves, which were taken at -80 °C, were transferred to cooled eppendorfs with the help of liquid nitrogen and crushed into powder with the help of a spatula. 1 ml of extraction buffer (100mM Tris-HCl [pH 8.0], 20 mM EDTA, 1.4 M NaCl, 0.2% (v/v) β-mercaptoethanol and 2% (w/v) CTAB) was added to the samples, and the mixture was mixed by vortex until homogeneous. After the material was completely dissolved, 5 µl of 10 mg/ml RNase concentration was added to the mixture and the mixture was incubated at 65°C for 45 min in a heat block. After incubation, the material was centrifuged at 4°C for 10 min at 12000 *g*. The supernatant was taken into a new tube, and an equal volume of chloroform: isoamyl alcohol (24:1, v/v) was added to the tube as the removed supernatant. The material was mixed with a vortex at high speed and centrifuged at 4°C and 12000g for 10 min. After centrifugation, the mixture was divided into 3 phases, with DNA at the top. The uppermost water-based DNA phase was taken into a new tube, and the DNA precipitated by adding an equal volume of pre-cooled isopropanol tubes. After gently turning the tubes upside down several times, they were kept at -20°C for at least 1 hour. Samples taken from 20°C were centrifuged at 4°C and 10000g for 5 min and collected pellets with DNA, and then supernatants were discarded. DNA pellets were washed with 1 ml of freshly brewed 70% (v/v) ethanol. The last centrifuge step for ethanol removal was repeated exactly. After the supernatants were removed, the DNA pellets were airflow-dried in a sterile cabinet to ensure that the ethanol was completely removed. DNA pellets were stored at –20°C after being 40ul dissolved in TE buffer containing 10 mM Tris-HCl (pH 8.0) and 1 mM EDTA. The concentration of DNA isolated from candidate transgenic plants was measured with NanoDrop, a micro-volume spectrophotometer. The quality of the DNAs was determined by agarose gel electrophoresis.

3.19. Total RNA extraction

Liquid nitrogen was utilized to chill the mortars and pestles that would be used for isolating RNA. After being extensively pulverized using these mortars and liquid nitrogen, *N. benthamiana* leaf samples were put into half-full, pre-cooled 2 ml tubes, and 1 ml of TRIzol (Invitrogen) solution was added. The tubes were then vortexed for fifteen

minutes. Following the vortex, the tubes were centrifuged for five minutes at 21000 g at room temperatures. A volume of around 800 µl of the supernatants was moved to fresh tubes, and 160 µl of chloroform was introduced into them. For three minutes, the mixture was allowed to incubate at room temperature. After that, the tubes were centrifuged for 15 min at 16000 *g* at 4°C. Following centrifugation, 400 µl of the RNA-containing water-based phase that had developed at the top was transferred into a fresh tube. Following a 3-minute incubation period at room temperature after adding 200 µl of chloroform to the supernatants, the mixtures were centrifuged at 21000g for 5 min at room temperature. Following this procedure, 400 µl of the upper phase was cautiously transferred to a clean tube and filled with the same volume of isopropanol. The tubes were thoroughly mixed several times and then allowed to incubate for ten minutes at room temperature. Following this time, the tubes were centrifuged for a maximum of 10 min at room temperature, and the supernatants that were produced were disposed of. Following a three-minute soak in 75% ethanol, the RNA pellets were allowed to come to room temperature. Following incubation, the tubes were centrifuged for 5 min at 21000 g at room temperatures., and the ethanol was removed during the process. To extract the last of the ethanol, a 15-second centrifuge was used. The tubes' mouths were then opened in the sterile cabinet, allowing air to remove all of the ethanol. Subsequently, the RNA pellets were mixed with 50 µl of DEPC water, the whole RNA was added, and the mixture was heated to 65°C for 10 min in order to dissolve the pellet.

3.20. Synthesis of single strand cDNA from total RNA

cDNA synthesis was performed from RNAs isolated after inflation. For this, the RevertAid First Strand cDNA Synthesis Kit (Catalog number: K1621) was used. The protocol included in the kit was used directly.

3.21. PCR after cDNA synthesis

The candidate gene (*GSH2*) of plants was confirmed by PCR and RT-PCR methods. DNA samples isolated from *N. benthamiana* leaves and single-stranded cDNA samples obtained from RNAs by reverse transcriptase enzyme were used as templates in the PCR method. PCR gene-specific and gRNA primers (Table 3.5), as stated below.

3.22. Gel extraction

Using a sterile cutting razor, the DNA fragment to be purified was removed from the agarose gel and transferred to a 1.5 ml microcentrifuge tube after adding 1 ml of Monarch Gel Dissolving Buffer. Incubated at 50°C, the agarose gel was inverted periodically until it was completely dissolved (usually 5-10 minutes). Place the column in the collection tube and load the sample into the column. 1 minute, 9000 g was also centrifuged, then supernatant. The column was reinserted into the collection tube, 200 µl of DNA Wash Buffer was added, and 1 min 9000 g was also centrifuged. Transfer the column to a clean 1.5 ml microfuge tube and add ≥ 6 µl of DNA Elution Buffer. Waited for 1 minute and finally, 1 minute to elute the DNA.

3.23. Next generation sequencing of possible mutations in *N. bethamiana* leaves after transfection

Following cloning and transfection, sequencing was performed by MGI sequencing method. At this stage, the service was purchased from Intergen (Turkey).

3.24. Measurement of GSH amount in *N. benthamiana* leaves

Fresh leaf samples were weighed on a precision balance and recorded. Each leaf sample was homogenized by adding 1.5 ml of 5% sulfosalicylic acid. The homogenate was centrifuged at 12,000 g for 20 min, and the supernatant was transferred to a new centrifuge tube. It was mixed with 1 mL 100 mM K-PO4 buffer (pH 7.0) containing 0.5 mM Na2 EDTA and 100 µL 3 mM 5-5'- dithiobis-2-nitrobenzoic acid (DTNB). After 5 min, absorbance was measured at 412 nm. Absorbance was expressed as Fresh Weight (FW) per gram fresh weight.

4. RESULTS

4.1. Preparation of Plant Transformation Vector

4.1.1. Vector isolation

E. coli bacteria, including the pKI1.1R vector, contain the spectinomycin antibiotic resistance gene. Amp-resistant pUC19 strain was cultured in an LB medium containing 50 mg/ml spectinomycin as a control LB medium containing 50 mg/ml spectinomycin medium, and in addition to this, the as seen in Figure 6, bacteria containing the pKI1.1R plasmid grew on spectinomycin antibiotic, while pUC19 bacteria, which are not resistant to this antibiotic, did not grow on this medium. This result clearly shows us that our antibiotic works at a concentration of 50 mg/ml and that our pKI1.1R plasmid is expressed in the strain.

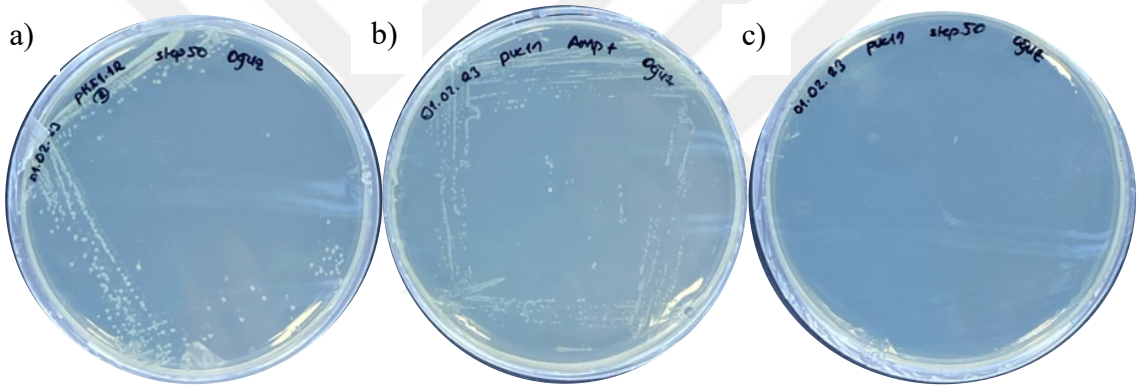

Figure 4.1. Growth images of *E.coli* bacteria on selective medium. (a) *E. coli* bacteria grown on spectinomycin antibiotic containing pKI1.1R plasmid. (b) *E. coli* bacteria containing pUC19 plasmid and amplified in Amp antibiotic. (c) *E. coli* bacteria containing pUC19 plasmid and grown in spectinomycin antibiotic.

The bacteria obtained after 16 hours of incubation were isolated using NEB's kit. After isolation, it was measured as 73,149 ng/ul. When the gel image was examined, it was seen that our plasmid was at the desired band length and did not contain genomic DNA contamination.

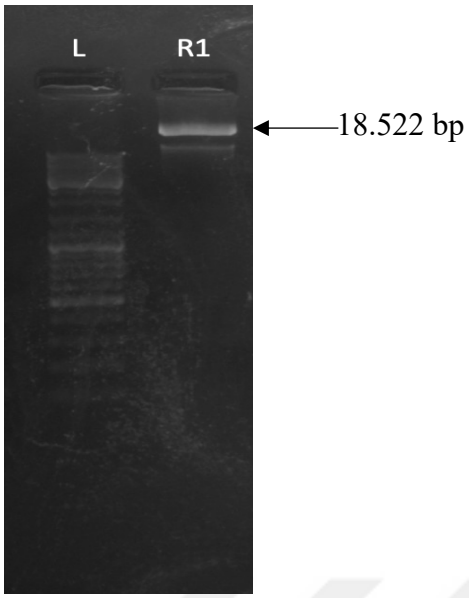

Figure 4.2. Image of the isolated pKI1.1R vector in 1% agarose gel after electrophoresis. The upper band represents DNA in a supercoiled conformation, while the lower band corresponds to DNA in a linear or circular form.

Table 4.1. Nanodrop measurements of isolated pKI1.1R vector.

Plasmid	**A_{260}**	**A_{260}/A_{230} nm**	**260/280 nm**	**Concentration (ng/µl)**
pKI1.1R	1,46	2,08	1,84	73,149

4.1.2. Cloning gRNA into the pKI1.1R vector

gRNAs were synthesized like primers by design but with specific modifications. The most fundamental of these is the phosphorylation step at the 5'-OH site. The main reason for this is that after the vector to be cloned is cut by enzyme digestion, there are phosphors at the 3' and 5' ends. However, in the cloning strategy, these phosphors are removed by the dephosphorylation step in 3.6. Thus, gRNAs synthesized with phosphorus can bind to this region correctly and easily. Another modification is that gRNAs are synthesized as two different primers. In order to be cloned, they need to be made into an oligoduplex structure. For this, the method described in section 3.7 was used. The ligation step was then performed. The results of this step by PCR and gel electrophoresis are shown in Figure 4.15.

4.1.3. Transformation of the ligation product to *E. coli* 10Beta and GV3101 *Agrobacterium* strains

The ligation product (cloned vector) was transformed into *E. coli* 10 Beta strain by heat shock and GV3101 *Agrobacterium* strain by electroporation. (Figure 4.3).

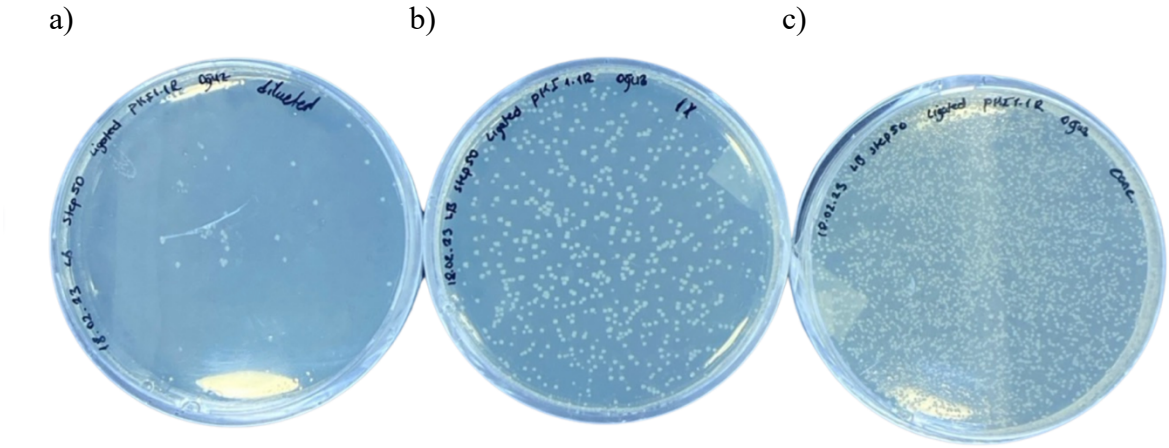

Figure 4.3. pKI1.1R-gRNA was transformed to 10-Beta *E. coli* strain a) 0.1x, b) 1x, c) 10x concentrations.

The results of the *E. coli* 10-Beta strain grown in a spectinomycin-containing medium after transformation are seen in Figure 4.3. As expected, colony formation was clearly observed at 10x concentration, less frequent at 1x concentration, and the least frequent at 0.1x concentration. Thus, validated transformation on selective media.

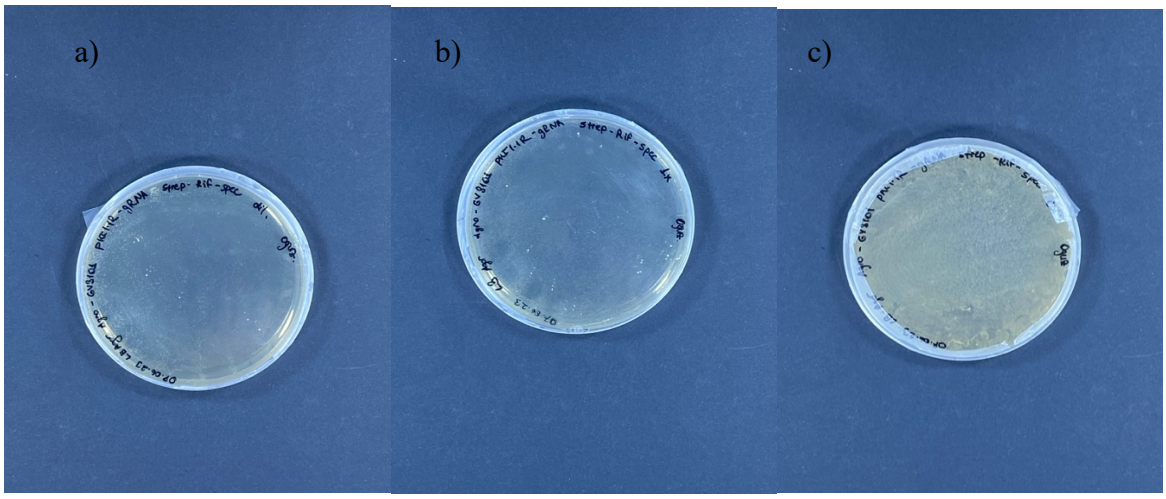

Figure 4.4. pKI1.1R-gRNA was transformed to GV3101 *A. tumefaciens* strain. a) 0.1x, b) 1x c) 10x concentrations.

The results of *A. tumefaciens* GV3101 strain grown on medium containing spectinomycin and streptomycin after transformation were shown in Figure 4.4. Thus, validated transformation on selective media.

4.1.4. Colony PCR

The first control after transformation was performed by backbone-specific PCR. For this purpose, primers specially designed for the Hygromycin antibiotic resistance gene in the vector were used.

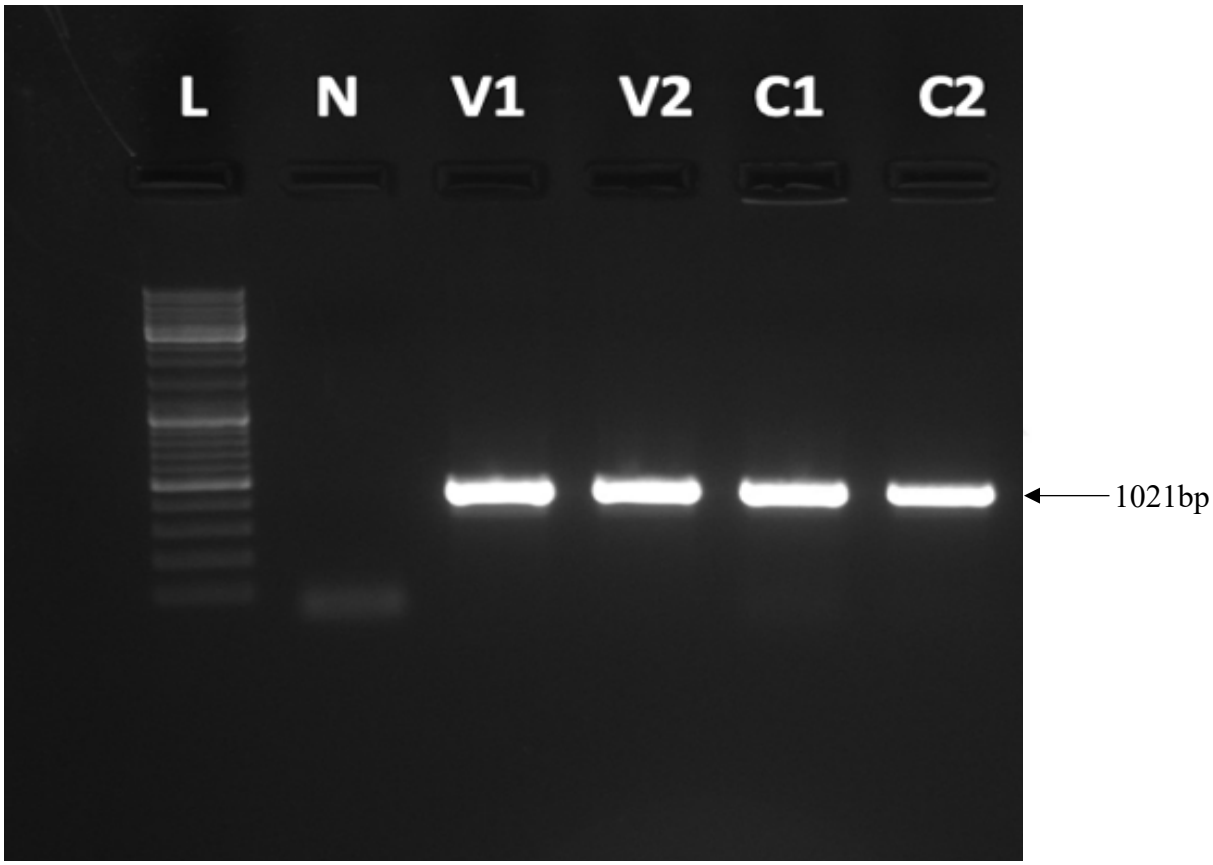

Figure 4.5. Post-PCR gel images of cloned but untransformed vector and transformed bacteria bacterial colonies. L: Ladder, N: Negative control, V: pKI1.1R-gRNA (Positive control), C1: 1st Colony, C2: 2nd Colony.

The length of the hygromycin antibiotic resistance gene in the plasmid was 1021 bp in both the positive control and the cloned and transformed bacteria and was confirmed by electrophoresis gel image. Based on this result, it was confirmed that the transformation of the vector into the 10-Beta strain of *E. coli* was successful.

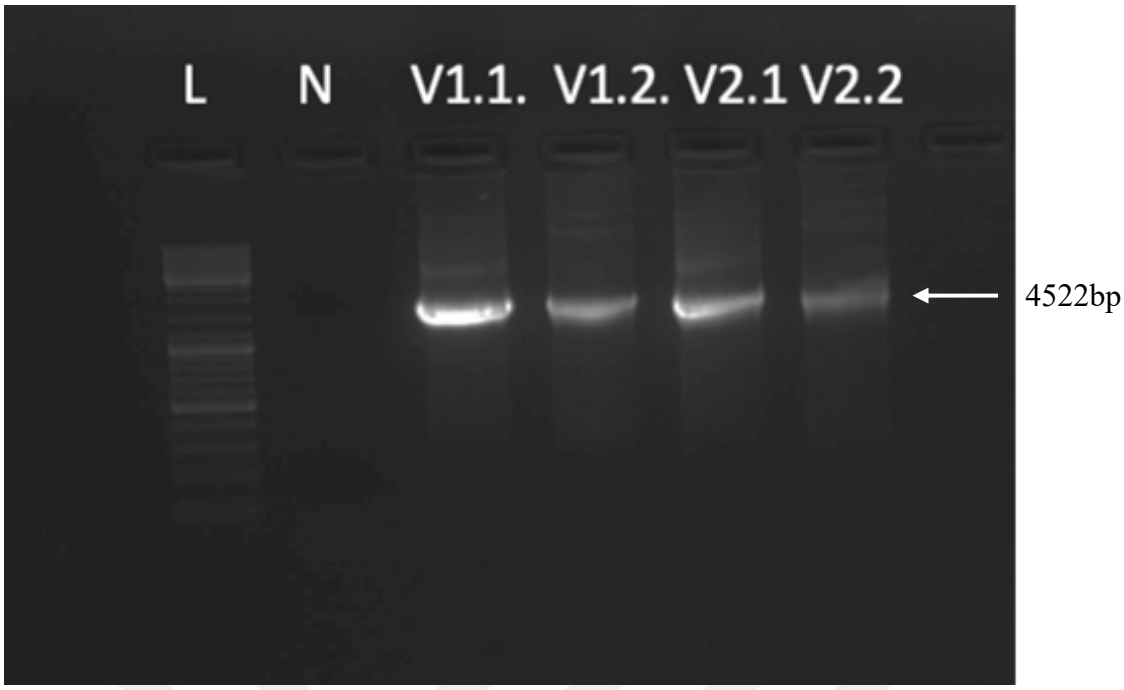

Figure 4.6. Insert specific PCR gel electrophoresis image after cloning and transformation L: Ladder, N: Negative control, V: Isolated plasmids after transformation.

The PCR result using Cas9R primer and gRNAF primer (Table 3.5) was specifically designed to include the Cas9 gene in the vector. The gel image shows the expected band length (Figure 4.6).

4.2. Validation of cloning by DNA sequencing

NGS was used to verify colonization. At this stage, the service was purchased from Intergen. The result is shown in Figure 4.7. The labelled region was found to coincide with our gRNA sequence. This allows us to verify that the gRNA is ligated into the pKI1.1R vector to be cloned in the desired orientation and at the desired site. In addition, it was confirmed that there were no non-specific cuts and, consequently, no mutations in the vector.

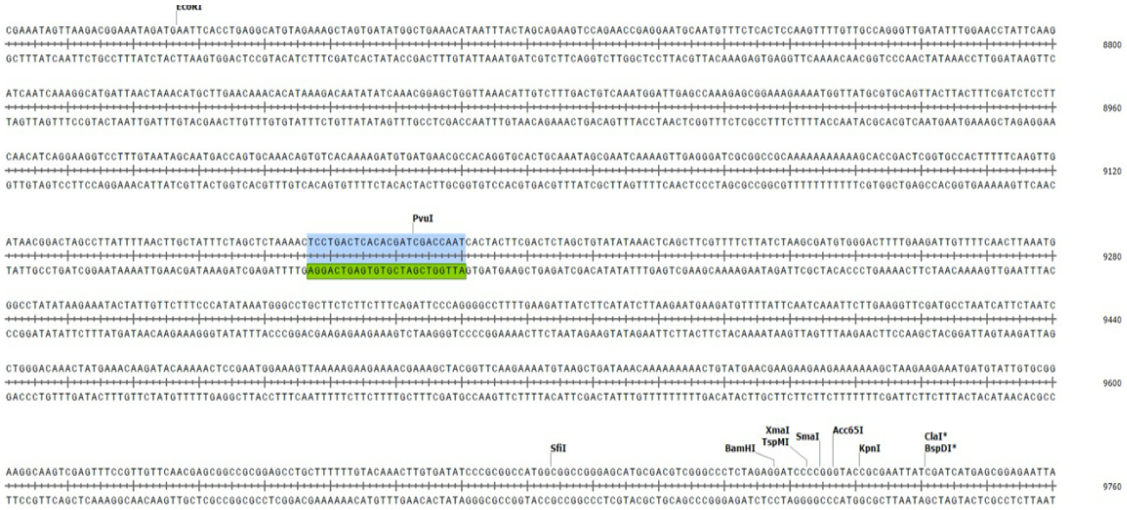

Figure 4.7. Sequence result of the pKI1.1R vector after ligation. Blue-Green region: shows the oligoduplex gRNA sequence.

4.3. Mobility Shift Assay

Electrophoresis Mobility Shift Assay (EMSA) was used to detect protein complexes with nucleic acids. In this case, protein and nucleic acid solutions were combined in certain proportions, and the resulting mixtures were subjected to agarose gel electrophoresis. In general, complexes formed by, the association of protein and nuclear acid, move through the gel more slowly than free nucleic acids. This is explained by the uptake mechanism [67]. Thus, the binding capacity of protein-nucleic acids was observed. After the N/P ratios specified in Table 3.6 were prepared, they were loaded with 0.8% agarose gel and carried out in 90V electrophoresis for 40 minutes.

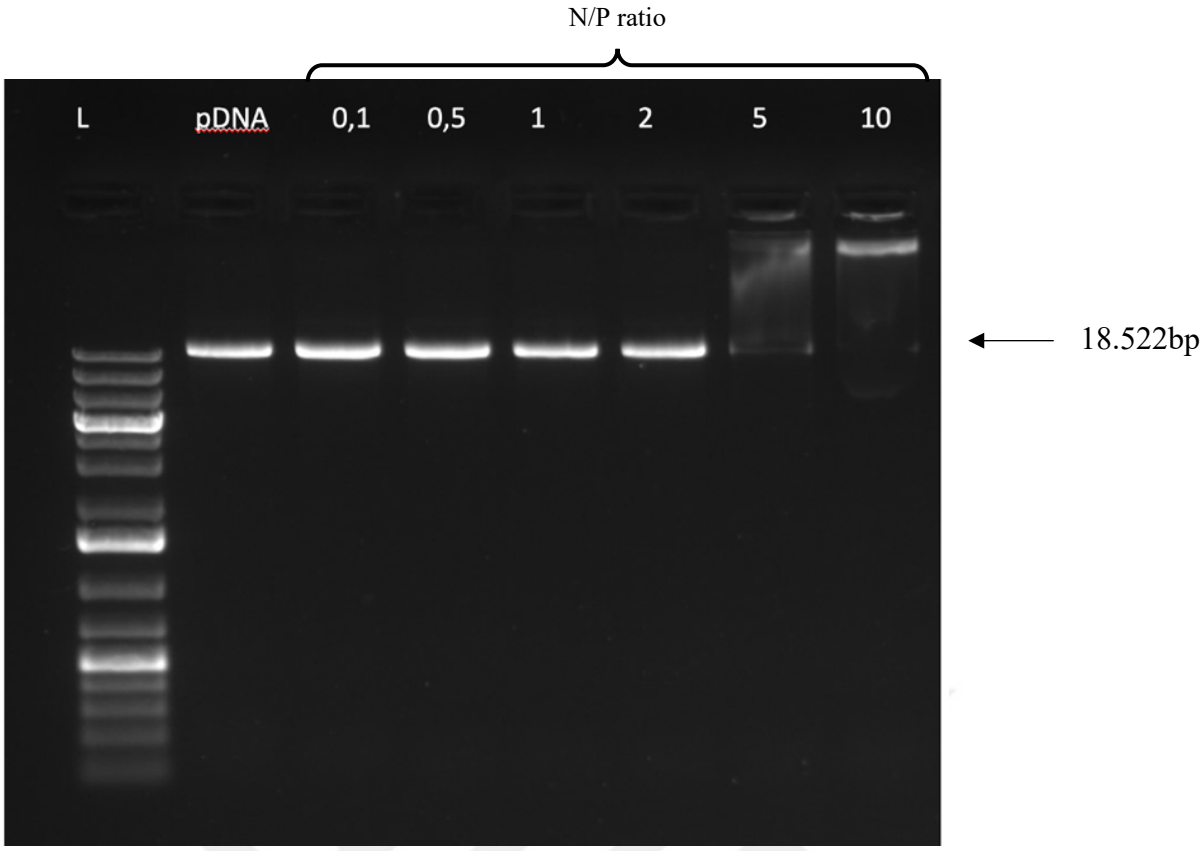

Figure 4.8. Gel image of mobility shift assay result L: Ladder, pDNA: Plasmid DNA, N/P ratio.

As can be seen in Figure 4.8, in CPP-pDNA complexes with N/P:0.1-0.5-1-2 ratios, there are unbound plasmids in the medium and uptake is low due to the low amount of CPP. At N/P:5 and N/P:10, the increase in the amount of CPP increased the uptake and the smear gel image showed that all plasmids in the medium were retained.

4.4. Zeta Potential Measurements

Zeta potential is often measured to estimate the surface charge and stability of nanomaterials because changes in these properties directly affect the biological activity of a particular nanoparticle. pDNA is negatively charged. The KLA-10 CPP used was positively charged.

Increasing the CPP concentration caused an increase in the positive surface charge (Figure 4.9). Above the N/P:10 ratio, the surface charge showed a positive result. All the negatively charged plasmids in the medium came together with a positive charge, and more CPP in the medium caused a positive charge. The increase in positivity is an indication that the amount of positively charged CPPs in the environment exceeds the amount of DNA and that the DNA that does not bind to the CPP does not remain in the environment. In the

Mobility Shift Assay result (Figure 4.8), there was a significant uptake at N/P:5 and N/P:10 ratios. Thus, the zeta-potential measurement and Mobility Shift Assay result are consistent with each other.

Figure 4.9. Zeta potential measurement of CPP-pDNA complexes prepared at different N/P ratios.

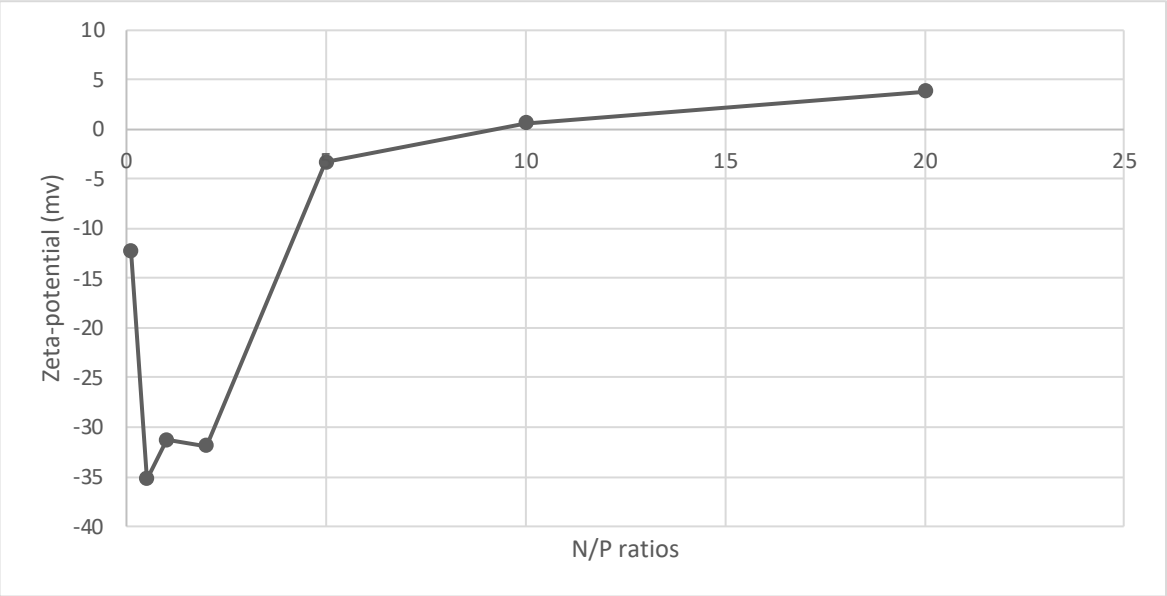

4.5. Investigation of the prepared pDNA/CPP complex and its effects on *N. benthamiana* leaves after transfection

When CPPs are infiltrated into plant cells at high concentrations, they cause toxic effects and necrosis in plants. Therefore, the toxic effects of CPP-pDNA complexes prepared at different N/P ratios on *N. benthamiana* leaves were investigated. The pDNA/CPP complex caused necrosis of *N. benthamiana* leaves after infiltration at ratios above N/P:1. To examine this on a time basis and at increasing concentration in Table 3.6, leaves were examined 3, 6 and 9 days after infiltration. On the third day after infiltration, CPP-pDNA complexes prepared at N/P:5 and N/P:10 caused visible necrosis of leaves. No necrosis was observed between N/P 0.1-2 ratios. At the end of the sixth day after infiltration, CPP-pDNA complexes infiltrated at N/P: 5 and N/P: 10 showed a high amount of necrosis on the infiltrated leaves, while CPP-pDNA complexes infiltrated between N/P: 0.1 and N/P: 2 showed very little necrosis on the leaf surface. After the ninth day post-infiltration, necrosis was observed in the infiltrated area at all N/P ratios, whereas at N/P 5 and N/P 10, a very high rate of necrosis was observed in all dispersed areas of the infiltration, including the infiltrated area.

Therefore, N/P 5 and N/P 10 ratios showed a very high toxic effect on the leaf and caused necrosis in the plants.

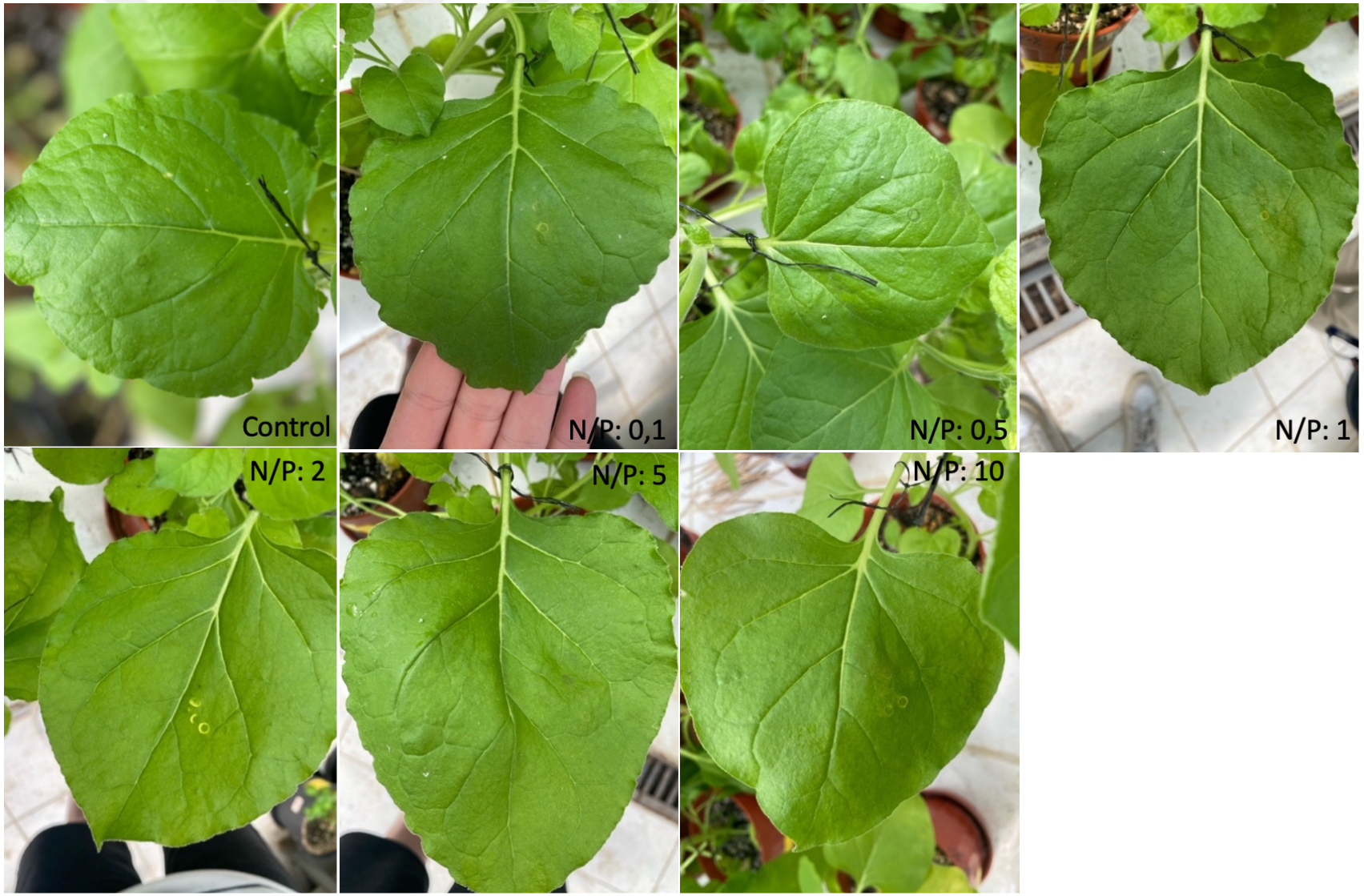

Figure 4.10. Images of CPP-pDNA complexes prepared according to Table 3.6 on *N. benthamiana* leaves after 3 days post infiltration.

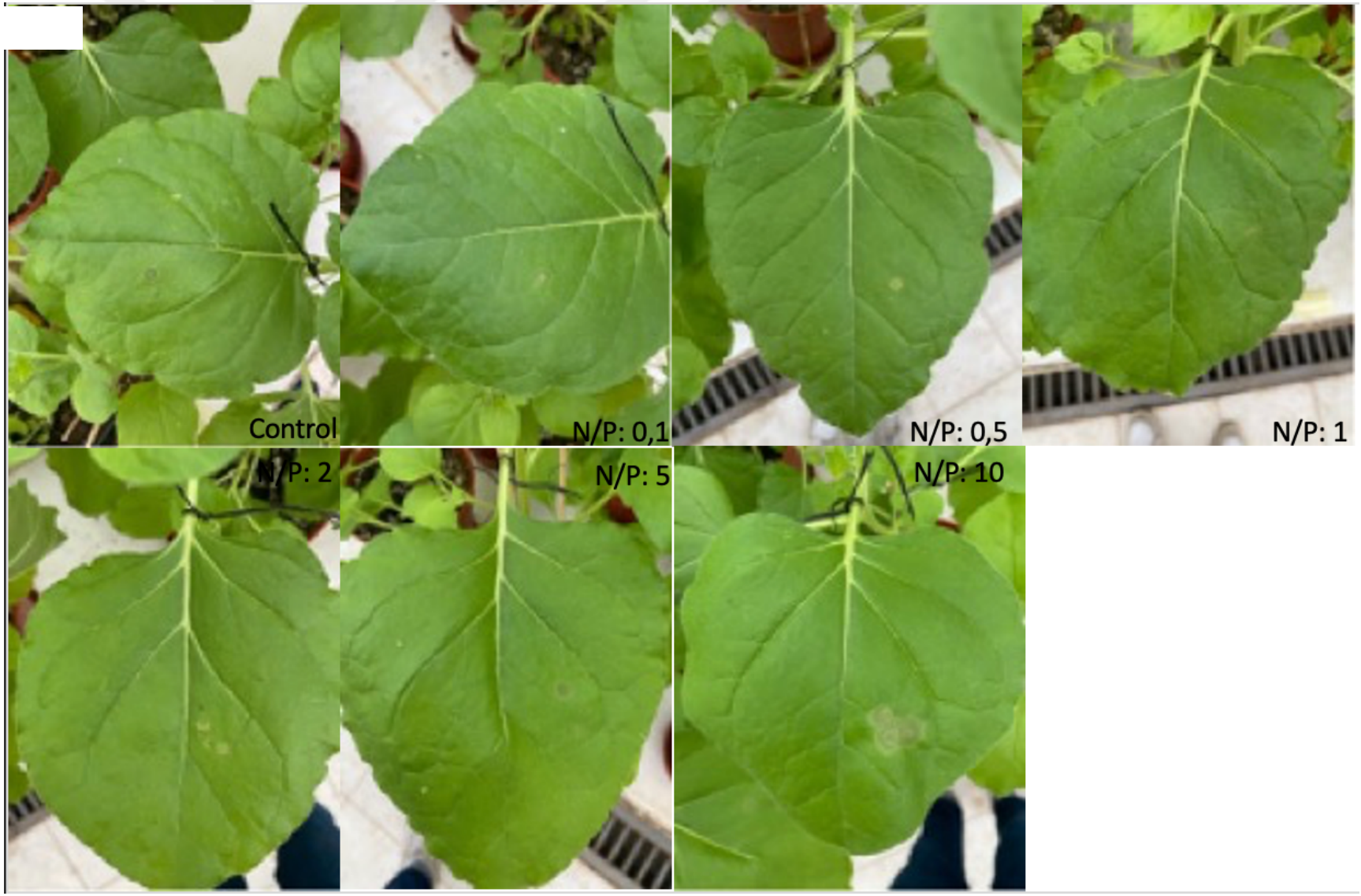

Figure 4.11. Images of CPP-pDNA complexes prepared according to Table 3.6 on *N. benthamiana* leaves after 6 days post infiltration.

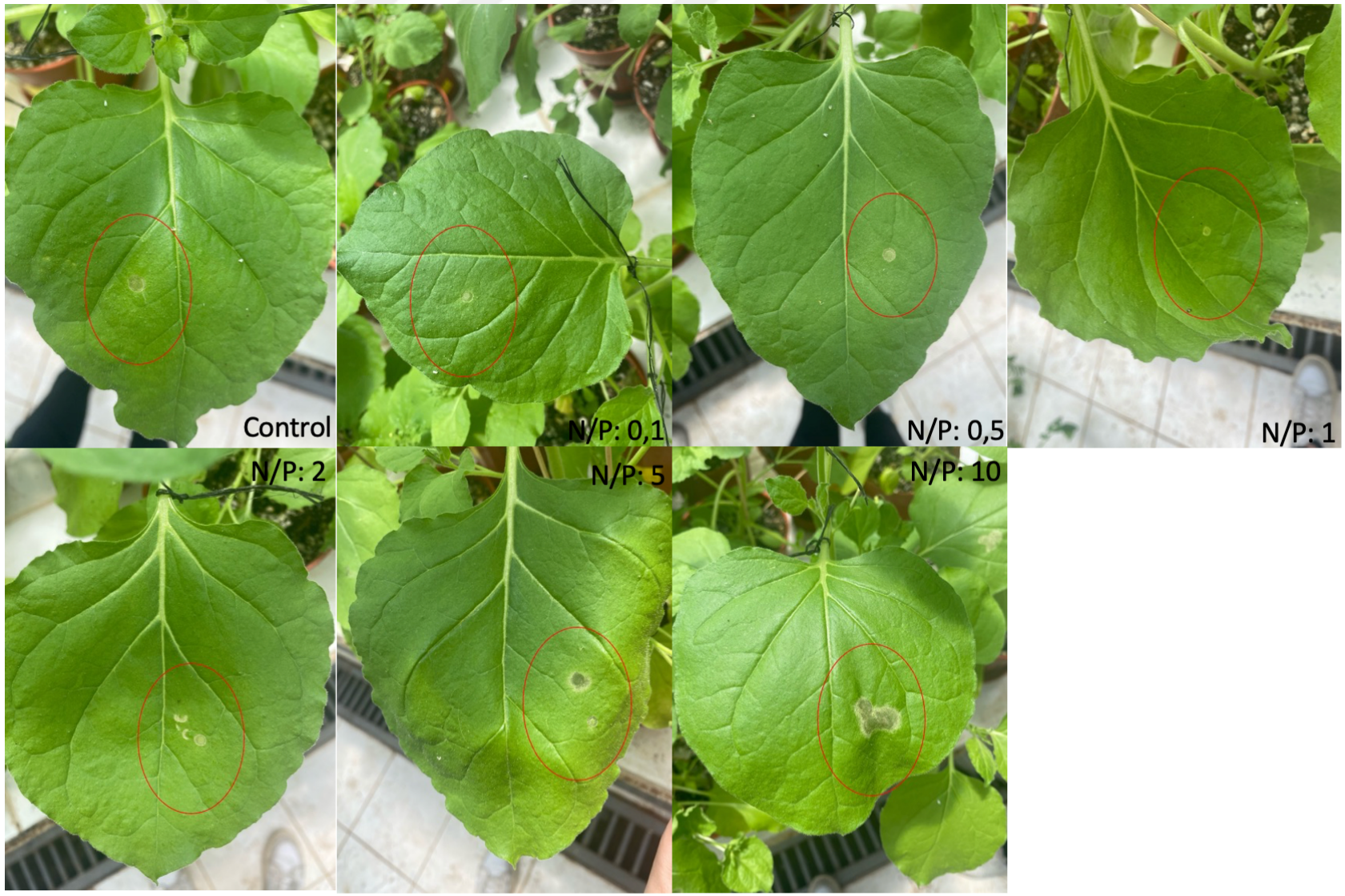

Figure 4.12. Images of CPP-pDNA complexes prepared according to Table 3.6 on *N. benthamiana* leaves after 9 days post-infiltration.

4.6. Comparison of N/P ratios with GFP vector

To evaluate the transfection efficiency between *Agrobacterium* transfection and transfection of CPP-pDNA complexes prepared at different N/P ratios and to examine the variation of this efficiency on a day-to-day basis. For this purpose, an expression vector containing a plant-specific GFP gene (pEAQ-GFP) was used. CPP-pDNAs were prepared at the N/P ratios given in Table 3.6 and two transfection systems were prepared by the *Agrobacterium* transformation method in 4.15. Then, *N. benthamiana* leaves were infiltrated with a needleless syringe. When the results were analysed, no clear GFP fluorescence was observed in both CPP-pDNA transfection and *Agrobacterium* transfection on the 3rd day after infiltration (Figure 4.13), while *Agrobacterium* infiltration was performed in the leaves on the 6th day after infiltration and a clear GFP fluorescence was observed after infiltration at N/P:1 N/P:2 and N/P:5 ratios (Figure 4.14). On the 9th day after infiltration, a clear GFP fluorescence was observed in both systems, especially in *Agrobacterium* infiltration and CPP-pDNA complexes with N/P:1 and N/P:2 ratios (Figure 4.15). However, as indicated in 4.11, necrosis was observed in CPP-pDNA complexes with N/P:5 and N/P:10 ratios at N/P:5. GFP fluorescence persisted in the infiltrated region at N/P:1 and N/P:2 ratios.

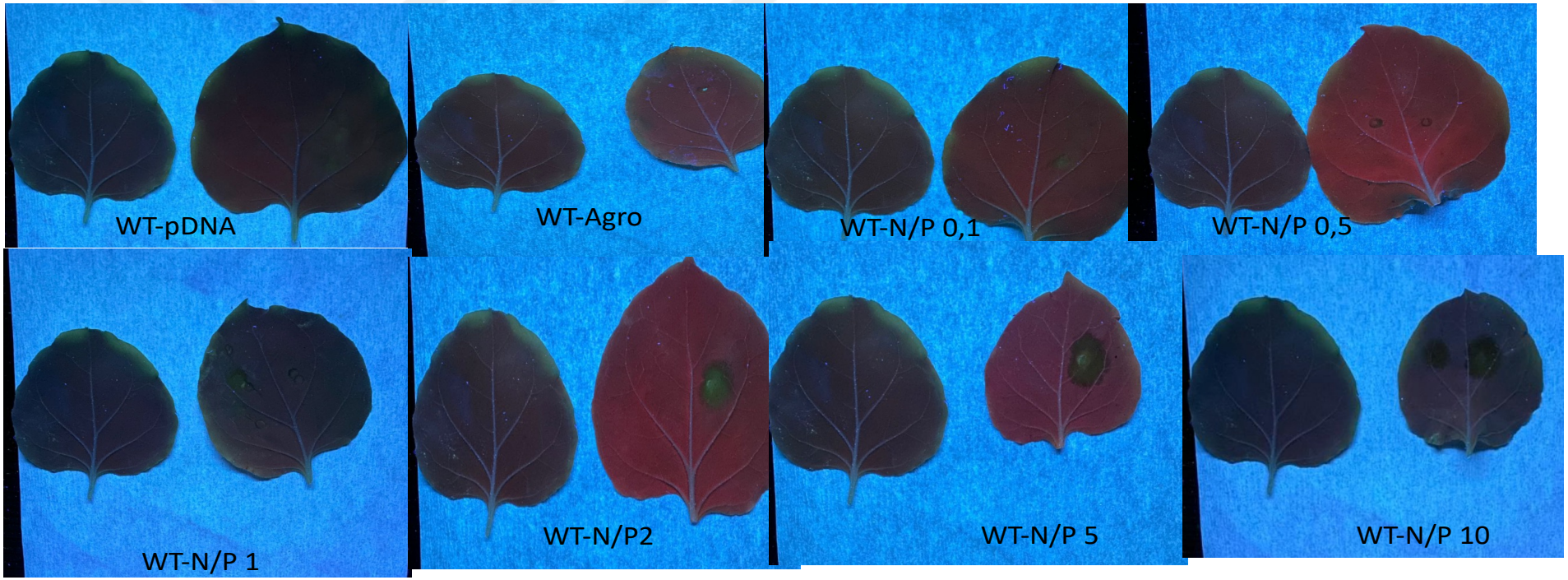

Figure 4.13. Images of *Agrobacterium* transfection containing pEAQ-GFP vector and CPP-pDNA complexes prepared at different N/P ratios after the third day of infiltration into *N. benthamiana* leaves.

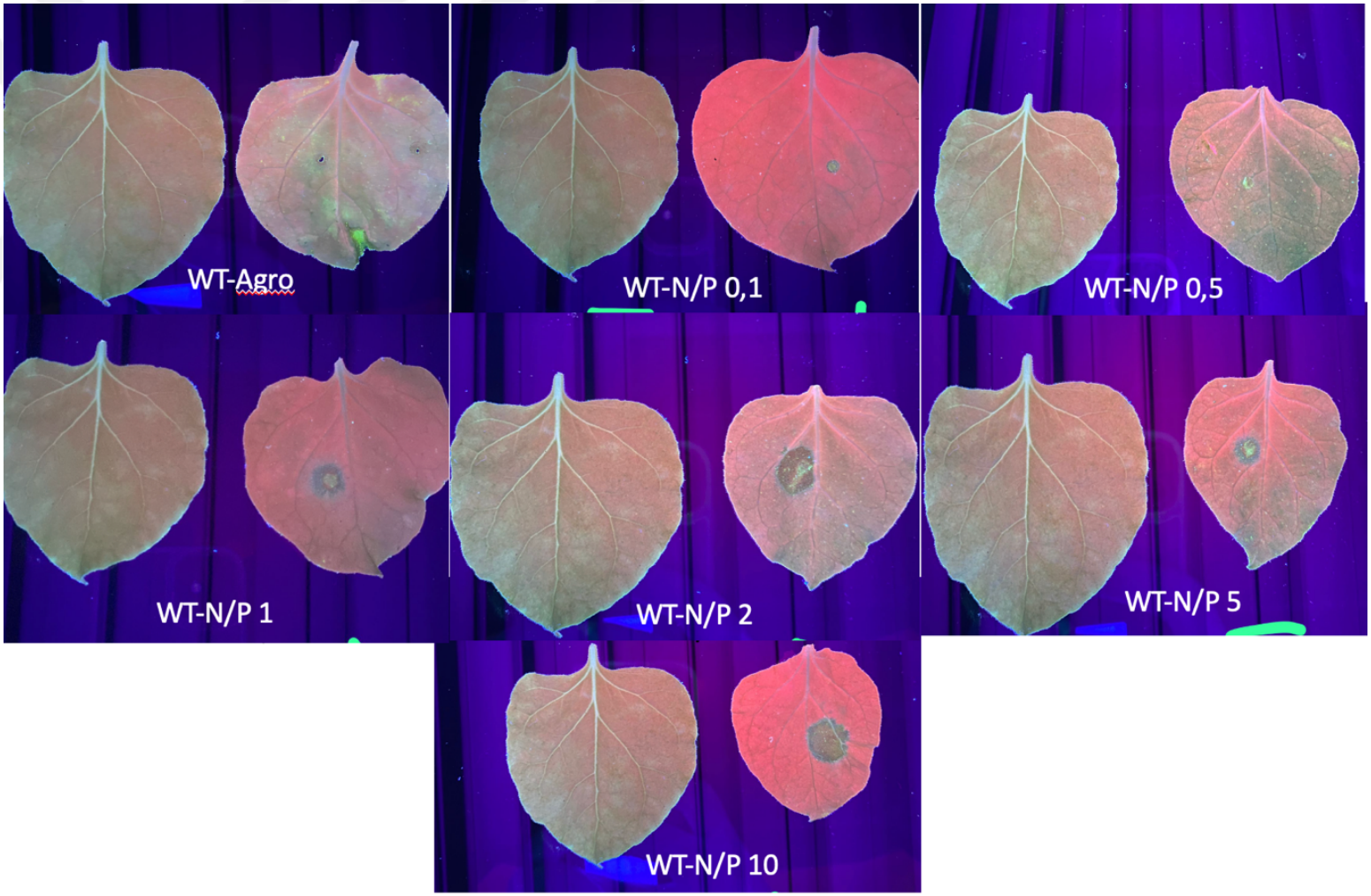

Figure 4.14. Images of *Agrobacterium* transfection containing pEAQ-GFP vector and CPP-pDNA complexes prepared at different N/P ratios after the sixth day of infiltration into *N. benthamiana* leaves.

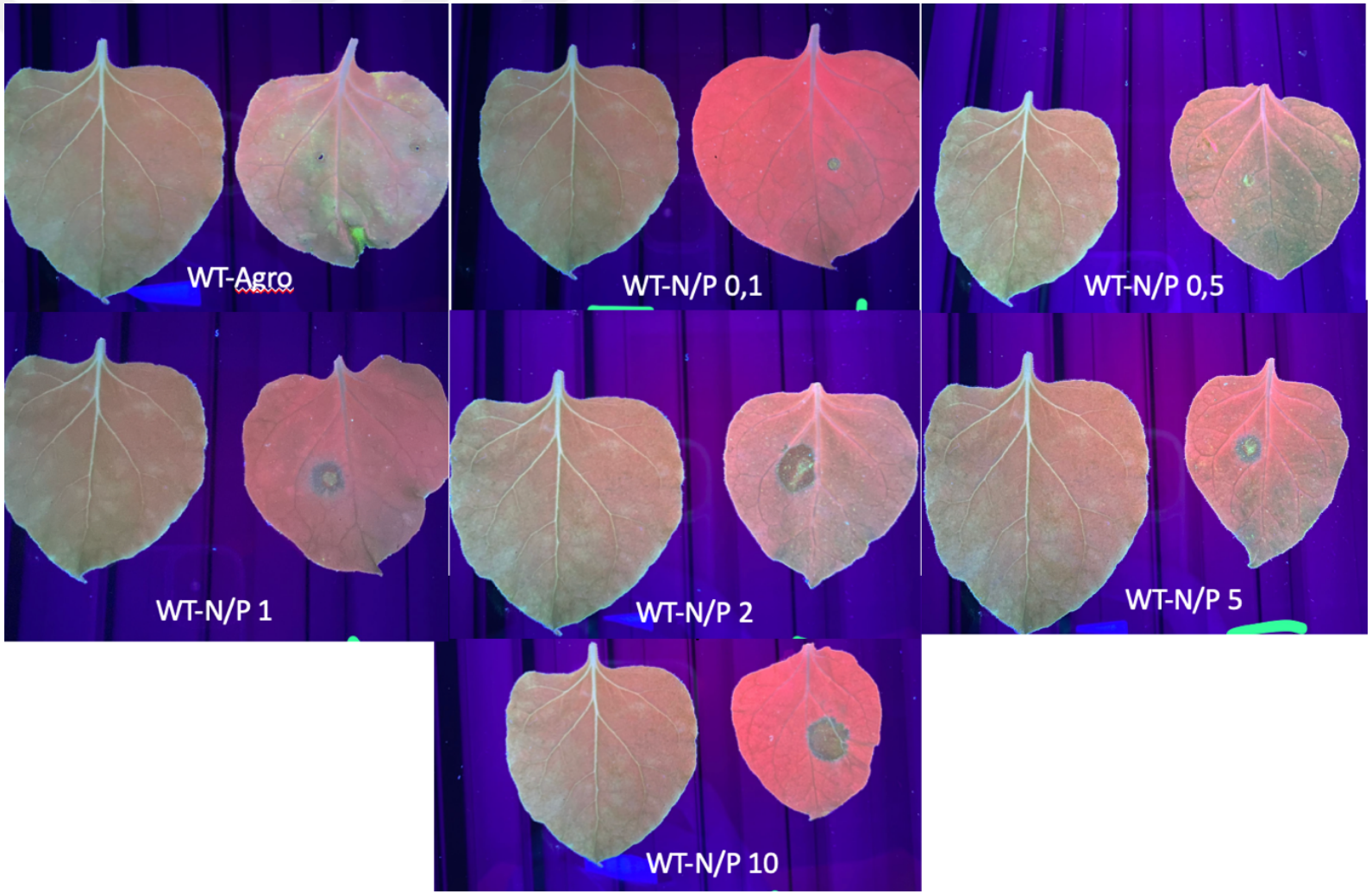

Figure 4.15. Images of *Agrobacterium* transfection containing pEAQ-GFP vector and CPP-pDNA complexes prepared at different N/P ratios after the ninth day of infiltration into *N. benthamiana* leaves

4.7. Investigation of the pDNA-CPP complex and the targeted *GSH2* gene after *Agrobacterium* infiltration

After RNA isolation from infiltrated plant leaves, RT-PCR was performed to confirm mutations in the gene with primers specifically designed for the *GSH2* gene. When the results were analyzed, a second band was observed in the leaves of plants infiltrated with pDNA-CPP complex and *Agrobacterium* transfection compared to WT. This was due to the appearance of two different bands in the gel image after the mutation or mixed profiles in the plant cells. As can be seen in Figure 4.16, it was clear that there was a band above 556 bp in the study for *GSH2* gene specific primers. This indicated that the repair mechanism was activated, and the probability of a random base filling after Cas9 activity was quite high. In the same study, the same heterogeneous pattern was observed with a gRNA forward primer fully complementary to the target site where the gRNA was thought to bind.

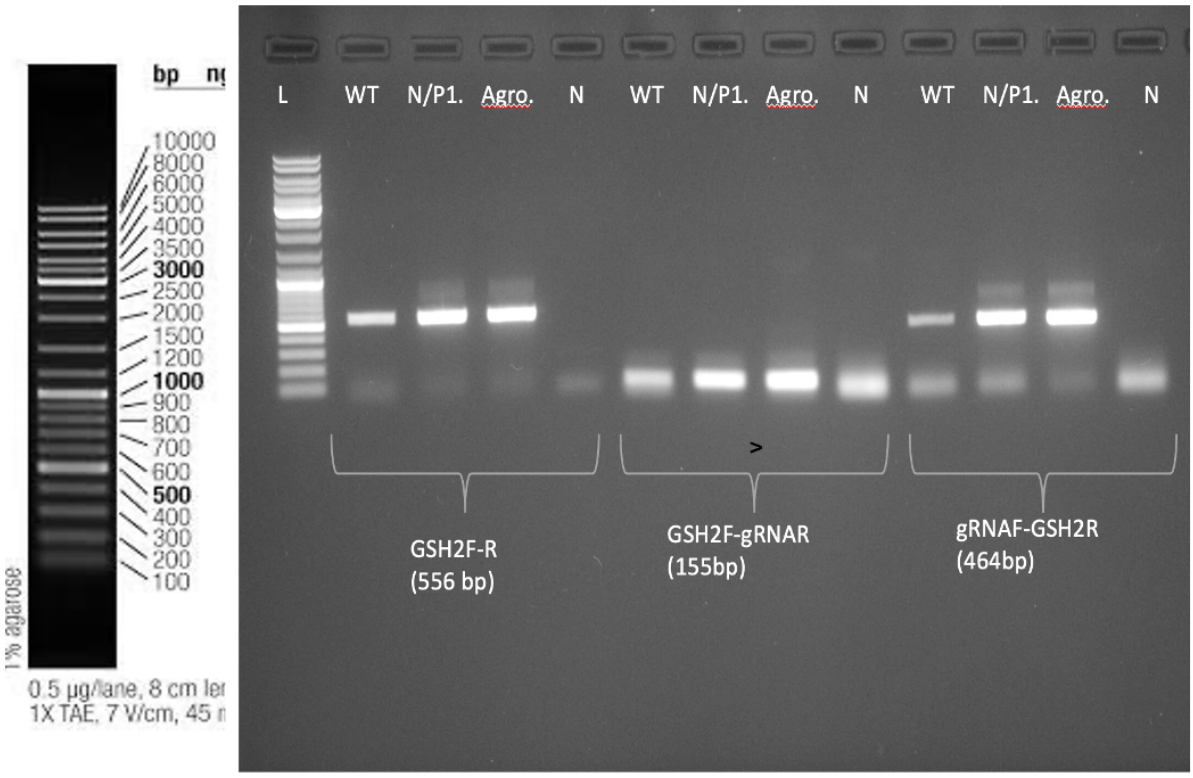

Figure 4.16. Agarose gel electrophoresis result after RT-PCR using different *GSH2* gene specific primers. WT: Wilde-type; Agro: DNA isolated from *Agrobacterium* infiltrated leaf sample; N/P: DNA isolated from CPP-pDNA infiltrated leaf sample.

In order to analyze these two bands seen in agarose gel electrophoresis, gel extraction was performed as upper and lower bands (Figure 4.16). After gel extraction, the same primers and PCR conditions were repeated with the same primers in order to visualize and sequence the two bands more distinctly. In the electrophoresis gel image made after PCR, the lower band is more dominant, although we separated them as upper and lower bands. The most significant difference was observed in the leaf with N/P:1 ratio (Figure 4.17).

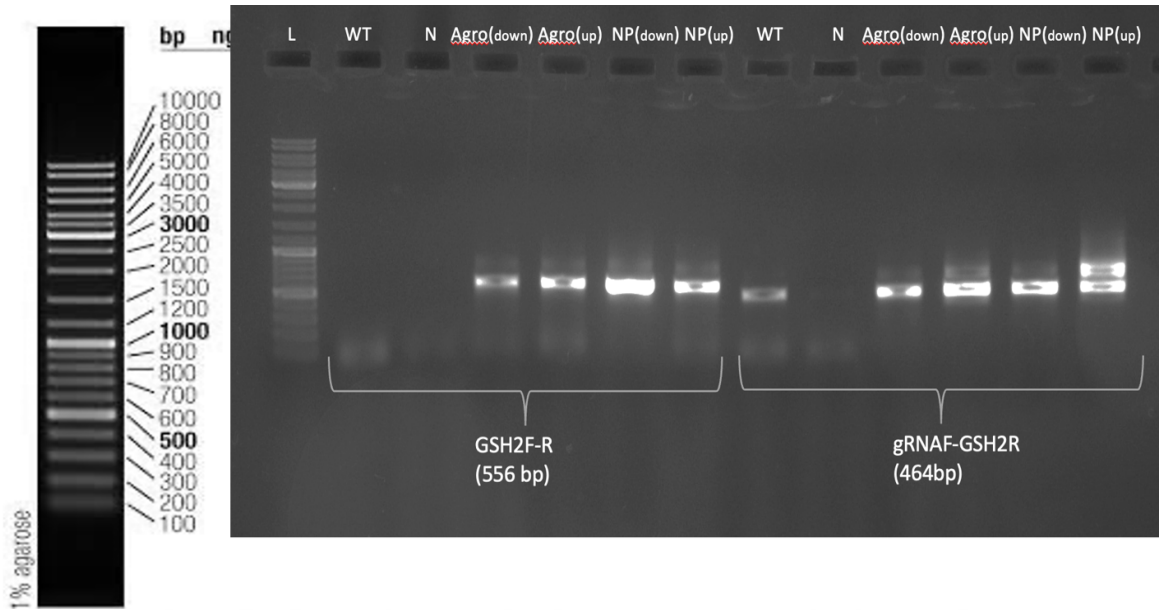

Figure 4.17. Gel electrophoresis image of the lower and upper bands isolated from N/P and *Agrobacterium* infiltrated leaves after reverse transcription, followed by gel extraction and PCR again,

4.8. GSH quantification

The GSH content of CPP-pDNA complexes with different N/P ratios and the *Agrobacterium* transfection system was analysed on a daily basis in comparison with WT. On day 3 after infiltration, there was no significant difference in both plant transfection systems. On the 6th day after infiltration, there was a significant decrease in GSH levels after infiltration of CPP-pDNA complex prepared in N/P:1 ratio and Agrobacterium compared to WT and had the lowest GSH content. When the percentage decrease was calculated, it was observed that N/P:1 had a very high value of 58% compared to day 3, followed by *Agrobacterium* transfection method with 44%. On the ninth day after infiltration, a dramatic increase in GSH was observed in all treatments compared to day 9 and WT (Figure 4.18).

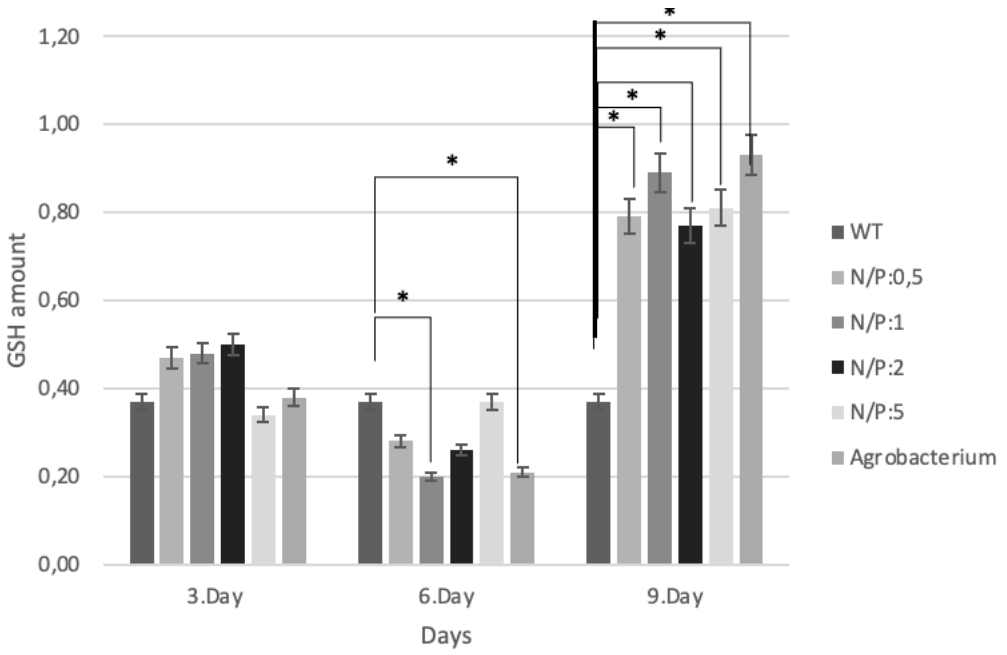

Figure 4.18. Results of GSH content determination after the first, third, sixth and ninth days of CPP-pDNA complex and *Agrobacterium* infiltration prepared at different N/P concentrations. Statistical analyses were performed using Python software (Python version 3.11.4, Anaconda, Inc. USA).

5. DISCUSSION

The free radical theory of aging emerged first with the studies carried out until today. This theory involves the accumulation of endogenous oxygen radicals produced in cells due to aging and the increase in aging-related diseases due to the decrease in the production of antioxidants produced in our cells to deal with these radicals [68]. In the following years, studies have shown the importance of an imbalance in the cellular reduction-oxidation state, called the redox state. The main reason why free radicals are so damaging to cells is that they have at least one unpaired electron at the very outside of their orbitals, making them highly reactive molecules. When these molecules cannot be detoxified in cells, oxidative stress occurs and cellular damage occurs as a result [69,70]. Oxidative stress in the neuronal system is a major problem because it underlies neurodegenerative diseases. This is mainly because ROS toxicity leads to protein misfolding, glia cell activation, mitochondrial dysfunction, and subsequent cellular apoptosis [71].

GSH is the most abundant antioxidant in many cells. Its most basic function is to maintain redox homeostasis in cells. Cell signaling, regulation of some enzyme activities, gene expression and cell differentiation/proliferation are other functions of GSH [72]. However, studies show that the production of GSH weakens with age and the amount in cells decreases day by day [73]. This is another indication of why neurodegenerative diseases are at very high levels with aging. The first solution that comes to mind is to supplement GSH from the outside, but this also has many drawbacks [74]. The most important of these is that the active or passive uptake of GSH in the cell is very low and insufficient [75]. Because of this, GSH primarily functions as an internal antioxidant and redox regulator; nevertheless, it is not directly or freely delivered across cells. Therefore, specialized transport systems or other processes may need to be included in circumstances when transfer across cells is required. Although various transportation systems and modifications have been made for this purpose, they have not yet been used effectively.

Today, the most effective method to increase the amount of intracellular GSH is the use of γ-glutamylcysteine (γ-GC), a precursor of GSH. γ-GC is an amino acid derivative that is derived from the combination of glutamic acid and cystine [18]. The γ-glutamyl cysteine ligase enzyme encoded by the *GSH1* gene takes place in this process. Then, with glutathione

synthase encoded by the *GSH2* gene, γ-GC and glycine come together to form GSH. Studies have shown that γ-GC can be used as a therapeutic against GSH deficiency. When γ-GC was given exogenously to the cell, an increase in GSH amount was observed [25]. It follows that the use of γ-GC as a treatment against GSH deficiency is not inevitable.

gRNA was specific for the *GSH2* gene of *N. benthamiana*, which was specifically designed for the pKI1.1R vector, a plant-specific CRISPR-Cas9 vector. AarI, a new generation cutting enzyme, was used in this thesis. This enzyme alone generates a sticky end. Then,a sticky end. Then, 10-Beta competent E. coli cells were transformed and isolated, and the pKI1.1R-gRNA vector was amplified. Then, for *Agrobacterium* transfection, the same vector was transformed into *Agrobacterium tumefaciens* strain GV3101 by electroporation. Another parameter was the control of CPP-pDNA stability. For this, performed Mobility Shift Assay and Zeta potential measurements. Accordingly, it was seen that a high degree of binding occurs at N/P:5 and N/P:10 ratios, and it was very difficult to move on the electrophoresis gel, and a smear image was formed. These results confirmed with zeta-potential results, and it was also shown that zeta-potential measurements at N/P:5 and N/P:10 values showed a positive electrical change. This is due to the fact that DNA is negatively charged, and the neutralization by the positive charge of CPP leads to a more dominant charge distribution of CPP.

CPP-pDNA complexes were then infiltrated into *N. benthamiana* leaves at N/P ratios of 0.1-10 and examined on the 3rd, 6th, and 9th day after infiltration. When the results were analyzed, no high amount of necrosis was observed in the range of 0.1-2 N/P, while a very high amount of necrosis was observed at N/P:5 and N/P:10. This was thought to be due to the high CPP ratio damaging the plant cells. For this reason, did not work with N/P:10 ratio in subsequent experiments.

To evaluate transfection and expression efficiency, plant specific GFP vector and CPP mixtures were infiltrated into plant leaves in the same proportions. When examined on the 3rd, 6th and 9th days after infiltration, no GFP fluorescence was observed on the 3rd day after infiltration, while GFP fluorescence was observed on the 6th and 9th day after infiltration. The most prominent fluorescence was observed at N/P:1, N/P:2 and N/P:5 ratios. Therefore, further studies were continued with N/P ratios of 0.5, 1, 2 and 5.

In the research paper "Rapid and Efficient Gene Delivery into Plant Cells Using Designed Peptide Carriers", transfection efficiency in *N. benthamiana* leaves was investigated with R9-Bp100, (KH)9-Bp100 and R9-Tat2 CPPs [64]. In the comparison between GFP vector (P35S-GFP) and CPP-pDNA complexes, the KLA-10 peptide used in this study showed similar efficacy.

RNA was isolated from *N. benthamiana* plants to screen the mutations. These RNAs were then reverse transcribed into cDNA by RT-PCR with gRNAF-R and GSH2F-GSH2R primers specific for *GSH2* gene and run on gel. When the gel image was analyzed, a band was observed in both studies with GSH2F-GSH2R and gRNAF-GSH2R primers compared to WT in N/P and *Agrobacterium* transfection. This band was 50-100 bp above the expected band above the expected image. Based on this, it was hypothesized that the mutation occurred, and extra bases were seen due to DNA repair mechanism in some plant cells.

GSH levels were determined from the infiltrated plants. Thus, it was aimed to observe the decrease in GSH levels after the targeted knock out in *GSH2* gene. When the results were analysed, no significant decrease was observed on day 3 after infiltration, while a dramatic decrease was observed on day 6. The most significant decrease was observed in N/P:1 and *Agrobacterium* transfection compared to WT. In percentage terms, the N/P:1 ratio accounted for a 58% decrease in GSH amount, which represents a very high GSH deficiency. Agrobacterium transfection method is followed by *Agrobacterium* transfection method with 44% decrease in GSH amount. Based on these results, it can be interpreted that *Agrobacterium* transfection method and CPP transfection method have the same efficiency. A dramatic increase in the amount of GSH was observed on the 9th day after infiltration. This is thought to be due to the activation of the GSH recovery mechanism mentioned in the literature and the effort to maintain GSH homeostasis [65].

Since classical biotechnology techniques require more time, labor, labor and financial resources, the need for an alternative solution that can be effective in a minimum period of time has emerged. At this point, genome editing technologies have gained importance in the field of molecular farming to produce high yields. In addition to this, the transportation of these biotechnological tools in an easier, practical, and safer way with new generation

transportation systems provides us with convenience, and it is predicted that it will be more effective than calcic transfection methods in the coming years.

6. CONCLUSION

Using CRISPR/Cas9 genome editing and CPP intracellular transport system, GSH production was successfully disrupted in *N. benthamiana* leaves by editing the *GSH2* gene encoding the enzyme glutathione synthase, which was involved in the GSH pathway and thus γ-GC accumulation was achieved. As mentioned in the literature section, this γ-GC is expected to be used therapeutically in Parkinson's and Alzheimer's diseases having GSH deficiency.

In this study, the new generation intracellular delivery systems were found to have the same effective effect when compared with conventional transfection systems and it is predicted that they will become even more effective with future modifications.

This study will shed light on molecular farming studies such as metabolite or product production in plants using CRISPR/Cas9 genome editing and CPP transfection system.

REFERENCES

[1] Li, J. F., Norville, J. E., Aach, J., McCormack, M., Zhang, D., Bush, J., Church, G. M., & Sheen, J. 2013. "Multiplex and homologous recombination-mediated genome editing in Arabidopsis and *Nicotiana benthamiana* using guide RNA and Cas9", Nature biotechnology, 31(8), 688–691.

[2] Shan, Q., Wang, Y., Li, J., Zhang, Y., Chen, K., Liang, Z., Zhang, K., Liu, J., Xi, J. J., Qiu, J. L., & Gao, C. (2013). Targeted genome modification of crop plants using a CRISPR-Cas system. *Nature Biotechnology 2013 31:8*, *31*(8), 686–688. https://doi.org/10.1038/nbt.2650

[3] Nekrasov, V., Staskawicz, B., Weigel, D., Jones, J. D. G., & Kamoun, S. (2013). Targeted mutagenesis in the model plant *Nicotiana benthamiana* using Cas9 RNA-guided endonuclease. *Nature Biotechnology*, *31*(8), 691–693. https://doi.org/10.1038/NBT.2655

[4] Woo, J. W., Kim, J., Kwon, S. il, Corvalán, C., Cho, S. W., Kim, H., Kim, S. G., Kim, S. T., Choe, S., & Kim, J. S. (2015). DNA-free genome editing in plants with preassembled CRISPR-Cas9 ribonucleoproteins. Nature Biotechnology, 33(11), 1162–1164. https://doi.org/10.1038/NBT.3389

[5] Islam, M. R., Kwak, J. W., Lee, J. soo, Hong, S. W., Khan, M. R. I., Lee, Y., Lee, Y., Lee, S. W., & Hwang, I. (2019). Cost-effective production of tag-less recombinant protein in *Nicotiana benthamiana*. *Plant Biotechnology Journal*, *17*(6), 1094–1105. https://doi.org/10.1111/PBI.13040

[6] Bally, J., Jung, H., Mortimer, C., Naim, F., Philips, J. G., Hellens, R., Bombarely, A., Goodin, M. M., & Waterhouse, P. M. (2018). The Rise and Rise of *Nicotiana benthamiana*: A Plant for All Reasons. *Https://Doi.Org/10.1146/Annurev-Phyto-080417-050141*, *56*, 405–426. https://doi.org/10.1146/ANNUREV-PHYTO-080417-050141

[7] Liu, Z. Q. (2020). Bridging free radical chemistry with drug discovery: A promising way for finding novel drugs efficiently. *European Journal of Medicinal Chemistry*, *189*, 112020. https://doi.org/10.1016/J.EJMECH.2019.112020

[8] Sharifi-Rad, M., Anil Kumar, N. v., Zucca, P., Varoni, E. M., Dini, L., Panzarini, E., Rajkovic, J., Tsouh Fokou, P. V., Azzini, E., Peluso, I., Prakash Mishra, A., Nigam, M., el Rayess, Y., Beyrouthy, M. el, Polito, L., Iriti, M., Martins, N., Martorell, M., Docea, A. O., … Sharifi-Rad, J. (2020). Lifestyle, Oxidative Stress, and Antioxidants: Back and Forth in the Pathophysiology of Chronic Diseases. *Frontiers in Physiology*, *11*, 552535.

[9] Valko, M., Leibfritz, D., Moncol, J., Cronin, M. T. D., Mazur, M., & Telser, J. (2007). Free radicals and antioxidants in normal physiological functions and human disease. *The International Journal of Biochemistry & Cell Biology*, *39*(1), 44–84. https://doi.org/10.1016/J.BIOCEL.2006.07.001

[10] Dinkova-Kostova, A. T., Talalay, P., Sharkey, J., Zhang, Y., Holtzclaw, W. D., Wang, X. J., David, E., Schiavoni, K. H., Finlayson, S., Mierke, D. F., & Honda, T. (2010). An exceptionally potent inducer of cytoprotective enzymes: elucidation of the structural features that determine inducer potency and reactivity with Keap1. *The Journal of Biological Chemistry*, *285*(44), 33747–33755. https://doi.org/10.1074/JBC.M110.163485

[11] Querfurth, H. W., & LaFerla, F. M. (2010). Alzheimer's Disease. *Https://Doi.Org/10.1056/NEJMra0909142*, *362*(4), 329–344. https://doi.org/10.1056/NEJMRA0909142

[12] Aoyama, K. (2021). Glutathione in the Brain. *International Journal of Molecular Sciences 2021, Vol. 22, Page 5010*, *22*(9), 5010. https://doi.org/10.3390/IJMS22095010

[13] Meister, A., & Anderson, M. E. (2003). GLUTATHIONE. *Https://Doi.Org/10.1146/Annurev.Bi.52.070183.003431*, *Vol. 52*, 711–760. https://doi.org/10.1146/ANNUREV.BI.52.070183.003431

[14] Richman, P. G., & Meister, A. (1975). Regulation of gamma-glutamyl-cysteine synthetase by nonallosteric feedback inhibition by glutathione. *Journal of Biological Chemistry*, *250*(4), 1422–1426. https://doi.org/10.1016/S0021-9258(19)41830-9

[15] Alton Meister, M. E. A. (1983). Glutathione. *Annual Review of Biochemistry*, *52*(1), 711–760.

[16] Iantomasi, T., Favilli, F., Marraccini, P., Magaldi, T., Bruni, P., & Vincenzini, M. T. (1997). Glutathione transport system in human small intestine epithelial cells. *Biochimica et Biophysica Acta (BBA) - Biomembranes*, *1330*(2), 274–283. https://doi.org/10.1016/S0005-2736(97)00097-7

[17] Anderson, M. E., & Meister, A. (1983). Transport and direct utilization of gamma-glutamylcyst(e)ine for glutathione synthesis. *Proceedings of the National Academy of Sciences*, *80*(3), 707–711. https://doi.org/10.1073/PNAS.80.3.707

[18] Braidy, N., Zarka, M., Jugder, B. E., Welch, J., Jayasena, T., Chan, D. K. Y., Sachdev, P., & Bridge, W. (2019). The precursor to glutathione (GSH), γ-glutamylcysteine (GGC), can ameliorate oxidative damage and neuroinflammation induced by Aβ40 oligomers in human astrocytes. *Frontiers in Aging Neuroscience*, *10*(JUL), 457374. https://doi.org/10.3389/FNAGI.2019.00177/BIBTEX

[19] Lu, S. C. (2013). Glutathione synthesis. *Biochimica et Biophysica Acta*, *1830*(5), 3143–3153. https://doi.org/10.1016/J.BBAGEN.2012.09.008

[20] Boyd-Kimball, D., Sultana, R., Mohmmad Abdul, H., & Butterfield, D. A. (2005). γ-glutamylcysteine ethyl ester-induced up-regulation of glutathione protects neurons against Aβ(1–42)-mediated oxidative stress and neurotoxicity: Implications for Alzheimer's disease. *Journal of Neuroscience Research*, *79*(5), 700–706. https://doi.org/10.1002/JNR.20394

[21] Grant, C. M., MacIver, F. H., & Dawes, I. W. (2017). Glutathione synthetase is dispensable for growth under both normal and oxidative stress conditions in the yeast Saccharomyces cerevisiae due to an accumulation of the dipeptide gamma-glutamylcysteine. *Https://Doi.Org/10.1091/Mbc.8.9.1699*, *8*(9), 1699–1707. https://doi.org/10.1091/MBC.8.9.1699

[22] Pocernich, C. B., & Butterfield, D. A. (2012). Elevation of glutathione as a therapeutic strategy in Alzheimer disease. *Biochimica et Biophysica Acta (BBA) - Molecular Basis of Disease*, *1822*(5), 625–630. https://doi.org/10.1016/J.BBADIS.2011.10.003

[23] Dalton, T. P., Chen, Y., Schneider, S. N., Nebert, D. W., & Shertzer, H. G. (2004). Genetically altered mice to evaluate glutathione homeostasis in health and disease. *Free Radical Biology and Medicine*, *37*(10), 1511–1526. https://doi.org/10.1016/J.FREERADBIOMED.2004.06.040

[24] Le, T. M., Jiang, H., Cunningham, G. R., Magarik, J. A., Barge, W. S., Cato, M. C., Farina, M., Rocha, J. B. T., Milatovic, D., Lee, E., Aschner, M., & Summar, M. L. (2011). γ-Glutamylcysteine ameliorates oxidative injury in neurons and astrocytes in vitro and increases brain glutathione in vivo. *NeuroToxicology*, *32*(5), 518–525. https://doi.org/10.1016/J.NEURO.2010.11.008

[25] Ferguson, G., & Bridge, W. (2016). Glutamate cysteine ligase and the age-related decline in cellular glutathione: The therapeutic potential of γ-glutamylcysteine. *Archives of Biochemistry and Biophysics*, *593*, 12–23. https://doi.org/10.1016/J.ABB.2016.01.017

[26] Belhaj, K., Chaparro-Garcia, A., Kamoun, S., Patron, N. J., & Nekrasov, V. (2015). Editing plant genomes with CRISPR/Cas9. *Current Opinion in Biotechnology*, *32*, 76–84. https://doi.org/10.1016/J.COPBIO.2014.11.007

[27] Zhang, B., Yang, X., Yang, C., Li, M., & Guo, Y. (2016). Exploiting the CRISPR/Cas9 System for Targeted Genome Mutagenesis in Petunia. *Scientific Reports 2016 6:1*, *6*(1), 1–8. https://doi.org/10.1038/srep20315

[28] Samanta, M. K., Dey, A., & Gayen, S. (2016). CRISPR/Cas9: an advanced tool for editing plant genomes. *Transgenic Research*, *25*(5), 561–573. https://doi.org/10.1007/S11248-016-9953-5

[29] Szczepek, M., Brondani, V., Büchel, J., Serrano, L., Segal, D. J., & Cathomen, T. (2007). Structure-based redesign of the dimerization interface reduces the toxicity of

zinc-finger nucleases. *Nature Biotechnology*, *25*(7), 786–793. https://doi.org/10.1038/NBT1317

[30] Gaj, T., Gersbach, C. A., & Barbas, C. F. (2013). ZFN, TALEN, and CRISPR/Cas-based methods for genome engineering. *Trends in Biotechnology*, *31*(7), 397–405. https://doi.org/10.1016/J.TIBTECH.2013.04.004

[31] Osakabe, Y., & Osakabe, K. (2015). Genome editing with engineered nucleases in plants. *Plant & Cell Physiology*, *56*(3), 389–400. https://doi.org/10.1093/PCP/PCU170

[32] Bhuyan, S. J., Kumar, M., Ramrao Devde, P., Rai, A. C., Mishra, A. K., Singh, P. K., & Siddiweue, K. H. M. (2023). Progress in gene editing tools, implications and success in plants: a review. *Frontiers in Genome Editing*, *5*, 1272678. https://doi.org/10.3389/FGEED.2023.1272678

[33] Boch, J., Scholze, H., Schornack, S., Landgraf, A., Hahn, S., Kay, S., Lahaye, T., Nickstadt, A., & Bonas, U. (2009). Breaking the code of DNA binding specificity of TAL-type III effectors. *Science*, *326*(5959), 1509–1512. https://doi.org/10.1126/SCIENCE.1178811

[34] Moscou, M. J., & Bogdanove, A. J. (2009). A simple cipher governs DNA recognition by TAL effectors. *Science (New York, N.Y.)*, *326*(5959), 1501. https://doi.org/10.1126/SCIENCE.1178817

[35] Pattanayak, V., Guilinger, J. P., & Liu, D. R. (2014). Determining the specificities of TALENs, Cas9, and other genome editing enzymes. *Methods in Enzymology*, *546*(C), 4. https://doi.org/10.1016/B978-0-12-801185-0.00003-9

[36] Baltes, N. J., & Voytas, D. F. (2015). Enabling plant synthetic biology through genome engineering. *Trends in Biotechnology*, *33*(2), 120–131. https://doi.org/10.1016/J.TIBTECH.2014.11.008

[37] Clasen, B. M., Stoddard, T. J., Luo, S., Demorest, Z. L., Li, J., Cedrone, F., Tibebu, R., Davison, S., Ray, E. E., Daulhac, A., Coffman, A., Yabandith, A., Retterath, A., Haun, W., Baltes, N. J., Mathis, L., Voytas, D. F., & Zhang, F. (2016). Improving cold

storage and processing traits in potato through targeted gene knockout. *Plant Biotechnology Journal*, *14*(1), 169–176. https://doi.org/10.1111/PBI.12370

[38] Char, S. N., Unger-Wallace, E., Frame, B., Briggs, S. A., Main, M., Spalding, M. H., Vollbrecht, E., Wang, K., & Yang, B. (2015). Heritable site-specific mutagenesis using TALENs in maize. *Plant Biotechnology Journal*, *13*(7), 1002–1010. https://doi.org/10.1111/PBI.12344

[39] Lee, H. B., Sundberg, B. N., Sigafoos, A. N., & Clark, K. J. (2016). Genome Engineering with TALE and CRISPR Systems in Neuroscience. *Frontiers in Genetics*, *7*(APR). https://doi.org/10.3389/FGENE.2016.00047

[40] Kumar, V., & Jain, M. (2015). The CRISPR–Cas system for plant genome editing: advances and opportunities. *Journal of Experimental Botany*, *66*(1), 47–57. https://doi.org/10.1093/JXB/ERU429

[41] Marraffini, L. A., & Sontheimer, E. J. (2010). Self versus non-self discrimination during CRISPR RNA-directed immunity. *Nature 2010 463:7280*, *463*(7280), 568–571. https://doi.org/10.1038/nature08703

[42] Bolotin, A., Quinquis, B., Sorokin, A., & Dusko Ehrlich, S. (2005). Clustered regularly interspaced short palindrome repeats (CRISPRs) have spacers of extrachromosomal origin. *Microbiology*, *151*(8), 2551–2561. https://doi.org/10.1099/MIC.0.28048-0/CITE/REFWORKS

[43] Mojica, F. J. M., Díez-Villaseñor, C., García-Martínez, J., & Soria, E. (2005). Intervening sequences of regularly spaced prokaryotic repeats derive from foreign genetic elements. *Journal of Molecular Evolution*, *60*(2), 174–182. https://doi.org/10.1007/S00239-004-0046-3/TABLES/6

[44] Pourcel, C., Salvignol, G., & Vergnaud, G. (2005). CRISPR elements in Yersinia pestis acquire new repeats by preferential uptake of bacteriophage DNA and provide additional tools for evolutionary studies. *Microbiology*, *151*(3), 653–663. https://doi.org/10.1099/MIC.0.27437-0/CITE/REFWORKS

[45] Rousseau, C., Gonnet, M., le Romancer, M., & Nicolas, J. (2009). CRISPI: a CRISPR interactive database. *Bioinformatics*, *25*(24), 3317–3318. https://doi.org/10.1093/BIOINFORMATICS/BTP586

[46] Bhaya, D., Davison, M., & Barrangou, R. (2011). CRISPR-Cas Systems in Bacteria and Archaea: Versatile Small RNAs for Adaptive Defense and Regulation. *Https://Doi.Org/10.1146/Annurev-Genet-110410-132430*, *45*, 273–297. https://doi.org/10.1146/ANNUREV-GENET-110410-132430

[47] Shan, S., Soltis, P. S., Soltis, D. E., & Yang, B. (2020). Considerations in adapting CRISPR/Cas9 in nongenetic model plant systems. *Applications in Plant Sciences*, *8*(1). https://doi.org/10.1002/APS3.11314

[48] Sánchez-León, S., Gil-Humanes, J., Ozuna, C. v., Giménez, M. J., Sousa, C., Voytas, D. F., & Barro, F. (2018). Low-gluten, nontransgenic wheat engineered with CRISPR/Cas9. *Plant Biotechnology Journal*, *16*(4), 902–910. https://doi.org/10.1111/PBI.12837

[49] Fichtner, F., Urrea Castellanos, R., & Ülker, B. (2014). Precision genetic modifications: a new era in molecular biology and crop improvement. *Planta*, *239*(4), 921–939. https://doi.org/10.1007/S00425-014-2029-Y

[50] Ma, X., Zhu, Q., Chen, Y., & Liu, Y. G. (2016). CRISPR/Cas9 Platforms for Genome Editing in Plants: Developments and Applications. *Molecular Plant*, *9*(7), 961–974. https://doi.org/10.1016/J.MOLP.2016.04.009

[51] Schiml, S., & Puchta, H. (2016). Revolutionizing plant biology: Multiple ways of genome engineering by CRISPR/Cas. *Plant Methods*, *12*(1), 1–9. https://doi.org/10.1186/S13007-016-0103-0/FIGURES/4

[52] Ding, Y., Li, H., Chen, L. L., & Xie, K. (2016). Recent Advances in Genome Editing Using CRISPR/Cas9. *Frontiers in Plant Science*, *7*(MAY2016), 703. https://doi.org/10.3389/FPLS.2016.00703

[53] Ceasar, S. A., Rajan, V., Prykhozhij, S. v., Berman, J. N., & Ignacimuthu, S. (2016). Insert, remove or replace: A highly advanced genome editing system using

CRISPR/Cas9. *Biochimica et Biophysica Acta (BBA) - Molecular Cell Research*, *1863*(9), 2333–2344. https://doi.org/10.1016/J.BBAMCR.2016.06.009

[54] Samanta, M. K., Dey, A., & Gayen, S. (2016). CRISPR/Cas9: an advanced tool for editing plant genomes. *Transgenic Research*, *25*(5), 561–573. https://doi.org/10.1007/S11248-016-9953-5

[55] Li, C., Unver, T., & Zhang, B. (2017). A high-efficiency CRISPR/Cas9 system for targeted mutagenesis in Cotton (Gossypium hirsutum L.). *Scientific Reports 2017 7:1*, *7*(1), 1–10. https://doi.org/10.1038/srep43902

[56] Klap, C., Yeshayahou, E., Bolger, A. M., Arazi, T., Gupta, S. K., Shabtai, S., Usadel, B., Salts, Y., & Barg, R. (2017). Tomato facultative parthenocarpy results from SlAGAMOUS-LIKE 6 loss of function. *Plant Biotechnology Journal*, *15*(5), 634–647. https://doi.org/10.1111/PBI.12662

[57] Malzahn, A. A., Tang, X., Lee, K., Ren, Q., Sretenovic, S., Zhang, Y., Chen, H., Kang, M., Bao, Y., Zheng, X., Deng, K., Zhang, T., Salcedo, V., Wang, K., Zhang, Y., & Qi, Y. (2019). Application of CRISPR-Cas12a temperature sensitivity for improved genome editing in rice, maize, and Arabidopsis. *BMC Biology*, *17*(1), 1–14. https://doi.org/10.1186/S12915-019-0629-5/FIGURES/7

[58] Zhang, B. (2015). MicroRNA: a new target for improving plant tolerance to abiotic stress. *Journal of Experimental Botany*, *66*(7), 1749–1761. https://doi.org/10.1093/JXB/ERV013

[59] Liu, X., Wu, S., Xu, J., Sui, C., & Wei, J. (2017). Application of CRISPR/Cas9 in plant biology. *Acta Pharmaceutica Sinica B*, *7*(3), 292–302. https://doi.org/10.1016/J.APSB.2017.01.002

[60] Bolhassani, A., Jafarzade, B. S., & Mardani, G. (2017). In vitro and in vivo delivery of therapeutic proteins using cell penetrating peptides. *Peptides*, *87*, 50–63. https://doi.org/10.1016/J.PEPTIDES.2016.11.011

[61] Thagun, C., Motoda, Y., Kigawa, T., Kodama, Y., & Numata, K. (2020). Simultaneous introduction of multiple biomacromolecules into plant cells using a cell-penetrating

peptide nanocarrier. *Nanoscale*, *12*(36), 18844–18856. https://doi.org/10.1039/D0NR04718J

[62] Numata, K., Horii, Y., Oikawa, K., Miyagi, Y., Demura, T., & Ohtani, M. (2018). Library screening of cell-penetrating peptide for BY-2 cells, leaves of Arabidopsis, tobacco, tomato, poplar, and rice callus. *Scientific Reports 2018 8:1*, *8*(1), 1–17. https://doi.org/10.1038/s41598-018-29298-6

[63] Ng, K. K., Motoda, Y., Watanabe, S., Othman, A. S., Kigawa, T., Kodama, Y., & Numata, K. (2016). Intracellular Delivery of Proteins via Fusion Peptides in Intact Plants. *PLOS ONE*, *11*(4), e0154081. https://doi.org/10.1371/JOURNAL.PONE.0154081

[64] Oehlke, J., Lorenz, D., Wiesner, B., & Bienert, M. (2005). Studies on the cellular uptake of substance P and lysine-rich, KLA-derived model peptides. *Journal of Molecular Recognition*, *18*(1), 50–59. https://doi.org/10.1002/jmr.691

[65] Badosa, E., Ferre, R., Planas, M., Feliu, L., Besalú, E., Cabrefiga, J., Bardají, E., & Montesinos, E. (2007). A library of linear undecapeptides with bactericidal activity against phytopathogenic bacteria. *Peptides*, *28*(12), 2276–2285. https://doi.org/10.1016/J.PEPTIDES.2007.09.010

[66] Wender, P. A., Mitchell, D. J., Pattabiraman, K., Pelkey, E. T., Steinman, L., & Rothbard, J. B. (2000). The design, synthesis, and evaluation of molecules that enable or enhance cellular uptake: Peptoid molecular transporters. *Proceedings of the National Academy of Sciences of the United States of America*, *97*(24), 13003–13008. https://doi.org/10.1073/PNAS.97.24.13003/

[67] Hellman, L. M., & Fried, M. G. (2007). Electrophoretic Mobility Shift Assay (EMSA) for Detecting Protein-Nucleic Acid Interactions. *Nature Protocols*, *2*(8), 1849. https://doi.org/10.1038/NPROT.2007.249

[68] Wickens, A. P. (2001). Ageing and the free radical theory. Respiration Physiology, 128(3), 379–391. https://doi.org/10.1016/S0034-5687(01)00313-9

[69] Aiken, C. T., Kaake, R. M., Wang, X., & Huang, L. (2011). Oxidative Stress-Mediated Regulation of Proteasome Complexes *. *Molecular & Cellular Proteomics*, *10*(5), R110.006924. https://doi.org/10.1074/MCP.M110.006924

[70] Ienco, E. C., Logerfo, A., Carlesi, C., Orsucci, D., Ricci, G., Mancuso, M., & Siciliano, G. (2011). Oxidative Stress Treatment for Clinical Trials in Neurodegenerative Diseases. *Journal of Alzheimer's Disease*, *24*(s2), 111–126. https://doi.org/10.3233/JAD-2011-110164

[71] Fulda, S., Gorman, A. M., Hori, O., & Samali, A. (2010). Cellular stress responses: Cell survival and cell death. *International Journal of Cell Biology* https://doi.org/10.1155/2010/214074

[72] Forman, H. J., Zhang, H., & Rinna, A. (2009). Glutathione: Overview of its protective roles, measurement, and biosynthesis. *Molecular Aspects of Medicine*, *30*(1–2), 1–12. https://doi.org/10.1016/J.MAM.2008.08.006

[73] Beiswanger, C. M., Diegmann, M. H., Novak, R. F., Philbert, M. A., Graessle, T. L., Reuhl, K. R., & Lowndes, H. E. (1995). Developmental changes in the cellular distribution of glutathione and glutathione S-transferases in the murine nervous system. *Neurotoxicology*, *16*(3), 425–440. https://europepmc.org/article/med/8584275

[74] Giustarini, D., Milzani, A., Dalle-Donne, I., & Rossi, R. (2023). How to Increase Cellular Glutathione. Antioxidants 2023, Vol. 12, Page 1094, 12(5), 1094. https://doi.org/10.3390/ANTIOX12051094

[75] Lash, L. H. (2009). Renal glutathione transport: Identification of carriers, physiological functions, and controversies. *BioFactors*, *35*(6), 500–508. https://doi.org/10.1002/BIOF.65